Author Manuscript

Author Manuscript

Author Manuscript

Author Manuscript

HHS Public Access

Author manuscript

Nature. Author manuscript; available in PMC 2019 June 12.

Published in final edited form as:

Nature. 2018 December ; 564(7735): 273–277. doi:10.1038/s41586-018-0774-y.

Disruption of a self-amplifying catecholamine loop reduces cytokine release syndrome

Verena Staedtke[1,2,7,*], **Ren-Yuan Bai**[3,7,*], **Kibem Kim**[1], **Martin Darvas**[4], **Marco L. Davila**[5], **Gregory J. Riggins**[3], **Paul B. Rothman**[6], **Nickolas Papadopoulos**[1], **Kenneth W. Kinzler**[1], **Bert Vogelstein**[1,*], and **Shibin Zhou**[1,*]

[1]Ludwig Center and the Howard Hughes Medical Institute at the Johns Hopkins Kimmel Cancer Center, Baltimore, MD, USA.

[2]Department of Neurology, Johns Hopkins University School of Medicine, Baltimore, MD, USA.

[3]Department of Neurosurgery, Johns Hopkins University School of Medicine, Baltimore, MD, USA.

[4]Department of Pathology, University of Washington, Seattle, WA, USA.

[5]H. Lee Moffitt Cancer Center and Research Institute, Tampa, FL, USA.

[6]Johns Hopkins University School of Medicine, Baltimore, MD, USA.

[7]These authors contributed equally: Verena Staedtke, Ren-Yuan Bai.

Abstract

Cytokine release syndrome (CRS) is a life-threatening complication of several new immunotherapies used to treat cancers and autoimmune diseases[1–5]. Here we report that atrial

Reprints and permissions information is available at http://www.nature.com/reprints.

Correspondence to: Verena Staedtke; Ren-Yuan Bai; Bert Vogelstein; Shibin Zhou.

Author contributions V.S. and R.-Y.B. originated the concept, designed and performed experiments, analysed the data and wrote the manuscript. K.K. and P.B.R. provided scientific advice. M.D. and M.L.D. provided animal models and scientific advice. B.V. and S.Z. designed the study, interpreted the data and wrote the manuscript. G.J.R., K.W.K. and N.P. contributed to the manuscript. All authors approved the final manuscript.

*vstaedt1@jhmi.edu; rbai1@jhmi.edu; vogelbe@jhmi.edu; sbzhou@jhmi.edu

Online content

Any methods, additional references, Nature Research reporting summaries, source data, statements of data availability and associated accession codes are available at https://doi.org/10.1038/s41586-018-0774-y.

Reviewer information *Nature* thanks K. Tracey and the anonymous reviewer(s) for their contribution to the peer review of this work.

Competing interests A patent application on CRS prevention listing V.S., R.-Y.B., G.J.R., K.W.K., N.P., S.Z. and B.V. as co-inventors has been provisionally filed by Johns Hopkins University. Under a licensing agreement between BVD Inc. and Johns Hopkins University, K.W.K., B.V. and S.Z. are entitled to a share of royalties managed by Johns Hopkins University. B.V., K.W.K. and NP are members of the Scientific Advisory Board of Sysmex and are founders of PapGene and Personal Genome Diagnostics. B.V. is also an advisor to Camden Partners. The terms of all these arrangements are managed by Johns Hopkins University in accordance with its conflict of interest policies. P.B.R. serves on Merck's board of directors.

Extended data is available for this paper at https://doi.org/10.1038/s41586-018-0774-y.

Supplementary information is available for this paper at https://doi.org/10.1038/s41586-018-0774-y.

Publisher's note: Springer Nature remains neutral with regard to jurisdictional claims in published maps and institutional affiliations.

Data availability

Source Data are provided for Figs. 1a, 2c, 3c, 4c, 5b and Extended Data Figs. 1a, 2a, b, 3a, b, 5a, 6a, 7a, 7d, 9h and 10d. The remaining datasets generated during this study are available from the corresponding authors on reasonable request. Unique materials such as the *C. novyi* strains are available on request to the corresponding authors. The transgenic mouse models and mouse CART constructs used in the study are made available through the original publishing authors.

Author Manuscript Author Manuscript Author Manuscript Author Manuscript

natriuretic peptide can protect mice from CRS induced by such agents by reducing the levels of circulating catecholamines. Catecholamines were found to orchestrate an immunodysregulation resulting from oncolytic bacteria and lipopolysaccharide through a self-amplifying loop in macrophages. Myeloid-specific deletion of tyrosine hydroxylase inhibited this circuit. Cytokine release induced by T-cell-activating therapeutic agents was also accompanied by a catecholamine surge and inhibition of catecholamine synthesis reduced cytokine release in vitro and in mice. Pharmacologic catecholamine blockade with metyrosine protected mice from lethal complications of CRS resulting from infections and various biotherapeutic agents including oncolytic bacteria, T-cell-targeting antibodies and CAR-T cells. Our study identifies catecholamines as an essential component of the cytokine release that can be modulated by specific blockers without impairing the therapeutic response.

Inflammation is crucial for immune defence against pathogens. However, when dysregulated, the cytokines that normally mediate protective immunity and promote recovery can cause a harmful systemic hyperactivated immune state known as cytokine release syndrome (CRS), which can lead to cardiovascular collapse, multiple organ dysfunction and death[1]. In addition to following infections by naturally occurring pathogens, CRS can be observed after biotherapeutic agents are administered to patients or to experimental animals, thereby seriously limiting the utility of these otherwise promising agents, which include oncolytic viruses and bacteria[3,6], recombinant lymphokines[5], natural and bispecific antibodies[2], and T cells designed to kill cancer cells[4].

The present study began with experiments employing the anaerobic spore-forming bacterial strain *Clostridium novyi*-NT to treat cancer[6]. *C. novyi*-NT spores germinate exclusively in hypoxic tumour tissues and can destroy them[6]. However, when high doses of spores were injected into very large tumours, a massive infection occurred and animals died within a few days with severe cytokine release due to a combination of tumour lysis and direct toxic effects of the bacteria (sepsis)[6] that was not reversed by the antibiotic metronidazole (Extended Data Fig. 1a). To mitigate this dose-limiting toxicity, we attempted to pre-treat mice with agents known to downregulate the inflammatory response[7,8]. Unfortunately, the anti-inflammatory agent dexamethasone and antibodies against TNF, IL-6 receptor (IL-6R) or IL-3 had limited effects on survival with only IL-6R blockade resulting in a significant but marginal improvement (Extended Data Fig. 1a).

We then engineered *C. novyi*-NT to secrete a number of anti-inflammatory proteins that might mitigate the bacteria-associated toxicity; atrial natriuretic peptide (ANP) was the only one that proved successful without compromising tumour lysis. ANP is an endogenous peptide released by cardiac cells, and regulates fluid and electrolyte homeostasis[9]. It has also been shown to have anti-inflammatory properties through reduction of cytokine release induced by lipopolysaccharide (LPS) in mice[9]. To investigate whether ANP could protect mice from severe bacterial infections such as those caused by *C. novyi*-NT, we engineered *C. novyi*-NT to express and secrete ANP by stably integrating an expression cassette of ANP with a signal peptide into the *C. novyi*-NT genome using the group II intron targeting[10]. Selected *C. novyi*-NT clones were characterized for ANP expression, biological activity and

Author Manuscript Author Manuscript Author Manuscript Author Manuscript

growth patterns in vitro (Extended Data Fig. 1b–d), and the clone with the highest expression of ANP (called 'ANP-*C. novyi*-NT', 1–29) was studied further.

One dose of ANP-*C. novyi*-NT spores injected into subcutaneously implanted CT26 tumours resulted in robust germination and tumour regression. Plasma levels of ANP and cyclic GMP (cGMP) in mice injected with ANP-*C. novyi*-NT were increased two to four times over that of mice injected with *C. novyi*-NT (Extended Data Fig. 1e, f). Strikingly, at similar efficiencies of germination and proliferation between the two strains (Extended Data Fig. 1g), more than 80% of the animals that received ANP-*C. novyi*-NT survived, 84% of which had complete tumour regression, whereas none of the mice treated with *C. novyi*-NT survived (Fig. 1a, upper and lower panel).

Mice injected with ANP-*C. novyi*-NT exhibited a noticeable reduction in tissue damage and inflammation. There were fewer infiltrating $CD11b^+$ myeloid cells in the liver, spleen and lungs (Fig. 1b, Extended Data Fig. 1h) and significant reductions in myeloid-derived cytokines (IL-1β, IL-6, MIP-2), chemoattractants (KC), and to a lesser degree, TNF and IFN-γ compared to mice treated with *C. novyi*-NT (Fig. 1c, Extended Data Fig. 1j). The latter cohort was also found to have an increased pulmonary permeability index (Extended Data Fig. 1i) and bone marrow myeloid hyperplasia (Fig. 1b, Extended Data Fig. 1h). Of interest, the diminished inflammatory response in mice treated with ANP-*C. novyi*-NT-treated was accompanied by markedly lower levels of circulating catecholamines (adrenaline, noradrenaline and dopamine) (Fig. 1d, Extended Data Fig. 1k). This finding was unrelated to changes in volume homeostasis, as estimated plasma volume and haematocrit were similar among the cohorts (Extended Data Fig. 1l, m).

We first determined whether the protective effect was due to expression of ANP by using ANP-releasing osmotic pumps implanted subcutaneously into mice before *C. novyi*-NT treatment. ANP delivered by pumps proved efficacious, with 75% of the mice surviving (Fig. 1a, upper panel), 77% of which exhibited complete tumour eradications. The other 23% of mice showed a robust but not curative response (Fig. 1a, bottom panel). Similar to ANP-*C. novyi*-NT, systemically delivered ANP also markedly reduced pro-inflammatory cytokines, catecholamines and tissue injury (Fig. 1 c, d, Extended Data Fig. 1h–k). Lastly, the effects of ANP were confirmed in another tumour model using subcutaneous implants of the glioblastoma cell line GL-261 in C56Bl/6 mice (Extended Data Fig. 2a).

We then investigated the mechanism underlying the protective effects of ANP. Previous studies link the anti-inflammatory properties of ANP to inhibition of phosphorylation of inhibitory κ B protein (IκB)[9]. Treatment with BMS-345541, a highly selective IκB kinase inhibitor[11], did not improve survival in mice treated with *C. novyi*-NT (Extended Data Fig. 2b), suggesting that ANP inhibits inflammation resulting from *C. novyi*-NT through mechanisms in addition to the NF-κB pathway. This prompted us to investigate the relationship between catecholamines and ANP.

Macrophages, which are major sources of inflammatory cytokines, secrete and respond to catecholamines through adrenergic receptors when exposed to inflammatory stimuli such as bacteria[12,13]. This in turn leads to increases in cytokine production, as shown in models of

Author Manuscript Author Manuscript Author Manuscript Author Manuscript

lung injury and experimental autoimmune encephalomyelitis[13,14]. Given the pleiotropic effects of catecholamines, we first determined which catecholamine contributed to the severity of inflammation injury by using subcutaneously implanted osmotic pumps that continuously released adrenaline, noradrenaline or dopamine into mice treated with LPS. Only mice with adrenaline pumps showed an exacerbated disease course, with increased mortality and higher levels of IL-6, TNF and KC compared to LPS-treated controls and mice treated with adrenaline only, in which an increase of cytokines was also observed (Extended Data Fig. 3a–d).

We next investigated the effect of ANP on catecholamine synthesis in stimulated mouse peritoneal macrophages. ANP inhibited the upregulated production of macrophageal catecholamines induced by LPS, which correlated with a reduction in levels of IL-6, TNF, MIP-2 and KC (Fig. 2a, b, Extended Data Fig. 3e). Notably, LPS in combination with adrenaline produced a markedly enhanced inflammatory response compared to that observed with each of the other agents, and this amplification was also inhibited by ANP (Fig. 2a, b, Extended Data Fig. 3e–g). Direct inhibition of catecholamine synthesis with α-methyltyrosine (metyrosine, MTR), which blocks the key target tyrosine hydroxylase (TH) and prevents the conversion of tyrosine to L-DOPA, greatly reduced levels of catecholamines produced by stimulated mouse macrophages (Fig. 2a, Extended Data Fig. 3e, f). Accordingly, cytokines released by macrophages were also diminished by MTR (Fig. 2b, Extended Data Fig. 3g). Comparable results were obtained with human U937-derived macrophages (Extended Data Fig. 4a, b).

To confirm that the production of catecholamines by macrophages drives the inflammatory response, we used peritoneal macrophages from mice with selective deletion of *Th* gene in LysM^{+} myeloid cells[15] (LysM^{cre} *Th*$^{fl/fl}$ or *Th*$^{\Delta LysM}$) resulting in significantly reduced TH expression levels (Extended Data Fig. 4c). Peritoneal macrophages with *Th* deleted showed reduced secretion of catecholamines and cytokines upon stimulation with LPS and adrenaline, which confirmed the role of autocrine catecholamine production in the amplification of the inflammatory cascade in macrophages (Extended Data Fig. 4d, e). Notably, the impaired ability to produce catecholamines led to a significant reduction in LPS-induced mortality and cytokine release in *Th*$^{\Delta LysM}$ mice (Fig. 2c–e).

MTR was found to have similar effects in vivo. Around 75% of mice injected with LPS survived when pre-treated with MTR compared to only 10% of control mice (Extended Data Fig. 5a). The effect of MTR on survival, catecholamines and cytokines was dose-dependent and 24-h serial plasma sampling showed sustained catecholamine and cytokine suppression (Extended Data Fig. 5a–e). To determine the relevant receptor, we used the inhibitors prazosin, RX 821002, metoprolol and ICI 118551 to block α_1, α_2, β_1 and β_2-adrenergic receptors, respectively[13]. Only blockade of α_1-adrenergic receptors by prazosin was effective in LPS-treated mice, achieving results similar to those obtained with MTR (Extended Data Fig. 6a–c).

To confirm the generality of these findings, we treated mice with MTR before the induction of CRS by infection with *C. novyi*-NT. Of the mice pre-treated with MTR, 85% survived, whereas only 8% of control mice survived (Extended Data Fig. 7a). As predicted, levels of

Author Manuscript Author Manuscript Author Manuscript Author Manuscript

catecholamines and cytokines were substantially reduced in the cohort pre-treated with MTR (Extended Data Fig. 7b, c).

Genetically engineered Gram-negative bacteria are also used in experimental therapies for cancer[16] and it is known that sepsis resulting from infection with Gram-negative bacteria differs from that caused by infection with Gram-positive bacteria, such as *C. novyi*-NT[17]. We therefore evaluated the effect of MTR in the caecal ligation and puncture (CLP) model, in which enteric bacteria, including many Gram-negative species cause polymicrobial peritoneal sepsis. MTR also significantly reduced the mortality from peritoneal sepsis: 22% of the mice survived the acute phase, whereas all control animals died (Extended Data Fig. 7d). When MTR was used in combination with the β-lactam antibiotic imipenem, more than two thirds of the mice survived CLP, whereas more than 90% of mice treated with imipenem alone died (Extended Data Fig. 7d). This result highlights that death from overwhelming bacterial infections is caused by both bacteria and host reaction (that is, CRS). To confirm that the detrimental host response was diminished by pre-treatment with MTR, we documented the expected effects of MTR on circulating catecholamines and cytokines (Extended Data Fig. 7e, f).

CRS is also observed after the administration of non-bacterial biotherapeutics and particularly those that activate T cells. For example, targeting the CD3 molecules of T cells with antibodies (muromonab-CD3, also known as OKT3) can mitigate autoimmunity and allograft rejection but leads to activation of T cells and CRS[18]. Accordingly, we found that cytokine release induced by anti-mouse-CD3 antibody 145–2C11 was accompanied by an upsurge of catecholamines in 5–6-month-old BALB/c mice (Fig. 3a–c, Extended Data Fig. 7g, h). Pre-treatment with MTR abrogated the increase in levels of catecholamines (Fig. 3a, Extended Data Fig. 7g) and several cytokines (IL-6, TNF, MIP-2, KC), whereas IL-2 and IFN-γ، were unaffected (Fig. 3b, Extended Data Fig. 7h). Pre-treatment with MTR also protected against CRS-associated mortality (Fig. 3c). Similar results were observed in mice with myeloid-specific deletion of *Th*; these mice were protected from excessive catecholamine and cytokine release, indicating that myeloid-derived catecholamines are an essential mediator for CRS (Fig. 3d, e).

Genetically engineered T cells that express tumour-directed chimaeric antigen receptors (CARTs) often induce life-threatening CRS. Blockade of IL-6R and IL-1R has been used to suppress CRS in patients and experimental animals[19–21]. To investigate whether CARTs generate and release appreciable amounts of catecholamines during tumour cell killing, human Burkitt's lymphoma-derived $CD19^+$ Raji cells were incubated in vitro with human CD19-directed CARTs (denoted as hCART19 cells; CD19scFv-CD28–4–1BB-CD3ζ), as detailed in the Methods. hCART19–Raji cell interaction caused the release of catecholamines and cytokines (IL-2, TNF, IFN-γ, MIP-1α) and both MTR and ANP abated this reaction (Fig. 4a, b, Extended Data Fig. 8a). To demonstrate adrenaline-driven autocrine induction, we added adrenaline to co-cultured Raji and hCART19 cells and observed an amplified catecholamine and cytokine response (Extended Data Fig. 8a–c). This response was strongly inhibited by the protein synthesis inhibitor cycloheximide (CHX), indicating that de novo protein synthesis is required (Extended Data Fig. 8d, e).

Author Manuscript Author Manuscript Author Manuscript Author Manuscript

To investigate the role of the catecholaminergic pathway on CART19-induced CRS in vivo, we injected Raji cells into sublethally irradiated[22,23] adult triple transgenic NSG-SGM3 (NSGS) mice. These mice express human myeloid supporting cytokines (IL3, GM-CSF, SCF) and can partially recapitulate CRS[22,24]. hCART19 cells were infused into Raji-bearing NSGS mice in two settings. In the first setting, hCART19 cells were infused at the half time of the median survival of untreated mice to establish a condition in which hCART19 cells would meet a high tumour burden and high risk for CRS (Fig. 4c–e, Extended Data Fig. 9a). We expected all these mice to die because hCART19 cells cannot rescue mice with high tumour burdens. In the second setting, hCART19 cells were infused at a third of the median survival time, when the mice had a relatively low tumour burden which allowed assessment of the anti-tumour response (Fig. 5a–d, Extended Data Fig. 9d). hCART19-treated mice with a high tumour burden died prematurely, with excessive levels of systemic catecholamines and cytokines at the time of death, including several human (*Hs*) T-cell-derived cytokines (*Hs*IL-2, *Hs*IFN-γ, and *Hs*TNF) and mouse (*Mm*) cytokines (*Mm*IL-6, *Mm*KC and *Mm*MIP-2) (Fig. 4c–e; Extended Data Fig. 9a–c). Pre-treatment with MTR significantly lowered the levels of circulating catecholamines and cytokines (*Hs*IFN-γ, *Hs*TNF, *Mm*IL-6, *Mm*KC and *Mm*MIP-2) but animals ultimately died, as expected, from progressive disease (Fig. 4c–e; Extended Data Fig. 9a–c). In mice with low tumour burdens, substantial anti-tumour effects of hCART19 cells were observed and more so in mice that received MTR (Fig. 5a, b; Extended Data Fig. 9d). Pre-treatment with MTR significantly lowered the increase of catecholamines, *Hs*TNF, *Mm*IL-6 and *Mm*KC in this model, and to a lesser degree *Hs*IFN-γ as well as *Hs*IL-2 (Fig. 5c, d; Extended Data Fig. 9e). We repeated these experiments with ANP, which yielded similar results (Extended Data Fig. 9f–h). Neither MTR nor ANP substantially interfered with hCART19 expansion (Extended Data Fig. 9i) or tumour clearance, and both were effective at preventing the cytokine release. Animals treated with the same amount of untransduced T cells (UT-T) did not show changes in survival, catecholamine or cytokine levels.

Because xenograft mouse models cannot fully predict the clinical behaviour of CART cells, we tested the effects of MTR and ANP in a syngeneic mouse model. C57Bl/6 mice engrafted with Eμ-ALL cells, a leukemia cell line derived from an Eμ-myc transgenic mouse to develop CD19-positive B cell acute lymphoblastic leukemia (B-ALL), were treated with CART19 cells directed against mouse CD19 (m1928z, mCART19), as detailed in Methods. Pre-treatment of mice with ANP or MTR did not affect the efficacy of the mCART19 cells in this model. However, the systemic release of catecholamines and cytokines was reduced by ANP and MTR, thereby confirming that these drugs may prevent the cytokine release while maintaining anti-tumour efficacy (Extended Data Fig. 10a–d).

A model illustrating the role of catecholamines in CRS is depicted in Fig. 5e. Our data, combined with previous studies[13,14,25], suggest that catecholamines enhance inflammatory injury resulting from bacterial and non-bacterial causes through a self-amplifying feed-forward loop in myeloid cells. Other catecholamine-producing cells, such as adrenal cells and T cells, in which stimulus-induced elevation of α_1- and α_2-adrenergic receptor levels have been reported[26], also probably participate in this feed-forward loop. Catecholamines secreted by such cells are synthesized by TH and act through α_1-adrenergic receptors expressed by immune cells. This circuit can be pharmacologically interrupted to modulate

Author Manuscript Author Manuscript Author Manuscript Author Manuscript

the inflammatory response. As MTR and prazosin are approved by the Food and Drug Administration for the treatment of hypertension, clinical translation of the findings is possible in clinical trials of agents whose application is restricted by CRS.

METHODS

Data reporting.

No statistical methods were used to predetermine sample size. All animal experiments were randomized; the investigators were blinded to the allocation, treatment and outcome assessment of experiments involving *C. novyi*-NT, CLP and anti-CD3.

Mice.

All animal experiments were performed in accordance with protocols approved by the Johns Hopkins Animal Care and Use Committee (ACUC) and relevant animal use guidelines and ethical regulations were followed. For subcutaneous CT26 tumour implantation, LPS and CLP experiments, female C57Bl/6 and BALB/C mice of 6–8 weeks were purchased from Harlan Laboratories. For anti-mCD3 treatment, female BALB/C mice of 5–6 months old were purchased form Harlan laboratories. For the CART19 treatment, NSG-SGM3 (NSGS) mice (stock number 013062) were purchased from the Jackson Laboratory.

LysM^{cre}-conditional *Th*-knockout mice.

LysM^{cre} mice were purchased from Jackson Laboratory (stock number 004781), in which a nuclear-localized Cre recombinase was inserted into the first coding exon of the lysozyme 2 (*Lyz2* or *LysM*) gene and expressed in the myeloid cell lineage (monocytes, mature macrophages and granulocytes)[15]. *Th* loxP/loxP ($Th^{fl/fl}$) mice were provided by M. Darvas at the University of Washington[27]. By crossing these two strains, LysM^{cre} $Th^{fl/fl}$ mice ($Th^{\Delta LysM}$) were produced as an experimental strain for LPS and anti-CD3 experiments and LysM^{cre} $Th^{+/+}$ mice ($Th^{+/+}$) were used as the Cre transgene control.

Chemicals and reagents.

Anti-mCD3 (145–2C11) and anti-mIL6 receptor (15A7) antibodies were purchased from BioXcell. Anti-mTNFα antibody (R023) was purchased from Sino Biological and anti-mIL3 antibody (MP2–8F8) was purchased from BD Biosciences. α-methyl-D,L-p-tyrosine methyl ester hydrochloride (Santa Cruz Biotechnology, SC-219470) is a soluble from of α-methyl-tyrosine (metyrosine, MTR), which is converted to α-methyl-tyrosine in vivo[28], whereas the less soluble α-methyl-tyrosine was purchased from Sigma (120693). LPS from *Escherichia coli* 0111:B4 (L2630), (−)-adrenaline (E4250), dopamine (H8502), noradrenaline (A7256), prazosin (P7791), metoprolol (M5391) and human ANP (A1663) were purchased from Sigma. RX 821002 (1324) and ICI 118551 (0821) were purchased from Tocris.

Strain engineering of *C. novyi*-NT.

The site-specific knock-in of human ANP in *C. novyi*-NT employed the TargeTron Gene Knockout System (Sigma), which is based on the retrohoming mechanism of group II introns[10]. The sequence of the human ANP cDNA was optimized for *Clostridium* codon

Author Manuscript Author Manuscript Author Manuscript Author Manuscript

usage as 5'-TCATTAAGAAGATCTTCATGTTTTGGAGGAAGAATGGATAGAATAGG AGCTCAATCAGGATTAGGATGTAATTCATTCAGATATTAA-3' coding for 28 AA (SLRRSSCFGGRMDRIGAQSGLGCNSFRY). The synthesized sequence was cloned into the shuttle vector pMTL8325. The construct included the *C. novyi* PLC signal peptide sequence under the control of the *C. novyi* flagellin promoter. Subsequently, the *MluI* fragment of the construct was subcloned into the vector pAK001 (pMTL8325-pJIR750ai Reverse-pFla-153 s-MCS-pThio-G1-ErmB) targeting the knock-in in the 153S site of *C. novyi*-NT genome. The *E.coli* CA434 strain containing the targeting construct was conjugated with *C. novyi*-NT and selected with polymyxin B/erythromycin (Sigma) under anaerobic condition. Colonies were selected and re-plated three times on non-selection plates and again on the erythromycin plate. Clones were tested first by PCR using EBS Universal and 153S-F primers. Positive clones were further tested by PCR with primers targeting the backbone of the vector to confirm the insert was integrated in *C. novyi* genome and with primers covering externally both sides of 153S to confirm the correct insertion. The propagation and sporulation of *C. novyi*-NT strains followed procedures described previously[29].

RNA extraction and quantitative PCR of *C. novyi*-NT strains.

For quantitative reverse transcription with PCR (RT–PCR), RNA of germinated *C. novyi*-NT strains were extracted using RiboPure Bacterial RNA Purification Kit (Ambion) and transcribed with SuperScript IV RT Kit (Invitrogen) as described[29]. Real-time PCR was performed using Maxima SYBR Green/ROX qPCR Master Mix (Thermo Fisher), targeting on the NT01CX1854 gene specific for geminating *C. novyi*-NT[29].

ANP measurement and cGMP assay.

ANP concentrations in the supernatant of ANP-*C. novyi*-NT culture and in mouse plasma were measured with an ELISA kit from Ray Biotech (EIAR-ANP-1) that recognizes both human and mouse ANP. ANP in the supernatant of ANP-*C. novyi*-NT culture were shown to have biological activity as described before[30]. Briefly, bacterial supernatants were applied to cultured bovine aortic endothelial cells (BAOEC, Cell Applications Inc.) for 3 min. cGMP concentrations were then measured in BAOEC lysates by the Direct cGMP ELISA Kit from Enzo following the manufacture's instruction.

Subcutaneous tumour models and *C. novyi*-NT therapy.

The colon cancer cell line CT26 was injected subcutaneously into the right flank of 6–8-week-old female BALB/C mice as described previously[6]. Tumour sizes were measured with a caliper and calculated as (L × W × H)/2. When tumours reached 600–900 mm^3 after about two weeks, 12×10^6 spores of *C. novyi*-NT or ANP-*C. novyi*-NT at 3×10^6 per μl were injected intratumourally into four central parts of the tumour with a 32G Hamilton syringe needle. The bacteria typically germinated in the tumours within 24 h, turning them necrotic. Hydration of the mice was supported by daily subcutaneous injections of 500 μl saline. Human ANP (Sigma) was dissolved in saline, loaded in mini-osmotic pumps (ALZET) with a release rate of 12 μg per day and implanted subcutaneously in the back of mice 12 h before the spore injection. Pumps loaded with saline served as controls. MTR was dissolved in PBS and injected intraperitoneally at 60 mg kg^{-1} per day for three days before the *C. novyi*

Author Manuscript Author Manuscript Author Manuscript Author Manuscript

injection to deplete catecholamines in storage. Two hours after the spore injection, 60 mg kg $^{-1}$ of MTR was injected intraperitoneally. For each of the next three days, intraperitoneal injections of MTR at 30 mg kg^{-1} were administered. Control groups were injected with PBS at the same time points.

Immunohistochemistry.

Immunostaining for CD11b was performed on formalin-fixed, paraffin-embedded sections on a Ventana Discovery Ultra autostainer (Roche Diagnostics) by S. Roy of JHU Oncology Tissue Services. Briefly, following dewaxing and rehydration on board, epitope retrieval was performed using Ventana Ultra CC1 buffer (6414575001, Roche Diagnostics) at 96 °C for 64 min. Primary antibody, anti-CD11b (1:8000 dilution; catalogue number ab133357, Abcam) was applied at 36 °C for 40 min. Primary antibodies were detected using an anti-rabbit HQ detection system (7017936001 and 7017812001, Roche Diagnostics) followed by Chromomap DAB IHC detection kit (5266645001, Roche Diagnostics), counterstaining with Mayer's haematoxylin, rehydration and mounting.

In vitro macrophage experiments.

Isolation of elicited macrophages from mouse peritoneum followed previously described procedures with minor modifications[31]. Four days before collection, 1 ml of 3% Brewer's thioglycollate medium (BD) was injected intraperitoneally in female 2–3-month-old BALB/c mice or 4–6-week-old conditional TH-knockout mice. Mice were killed by cervical dislocation and the skin of the belly was cut open without penetrating the muscle layer. Using a syringe with a 25G needle, 5 ml of cold PBS containing 5 mM EDTA was injected carefully into the peritoneal cavity. After massaging gently for 1–2 min, a 1-ml syringe without needle was used to extract the peritoneal contents containing residential macrophages. Cells were centrifuged at 400*g* for 10 min at 4 °C, re-suspended in DMEM/F12 medium supplemented with 1% FBS and antibiotics and distributed in 48-well plates at a concentration of 0.5×10^6 cells/well. After incubation at 37 °C for 2 h, cells were rinsed three times with 0.5 ml medium and then 250 µl of medium was added to each well. Ten minutes before the addition of LPS or adrenaline, MTR at 2 mM or ANP at 5 µg ml^{-1} was added to the cells. For stimulation, the cells were incubated for 24 h with LPS at 50 µg ml^{-1}. An initial solution of 3 mg ml^{-1} (−)-adrenaline was made with 0.1N HCl and subsequently diluted with PBS. To stimulate macrophages, they were exposed to adrenaline at 15 ng ml^{-1} for 24 h at 37 °C. After the incubation, supernatants were collected from the wells and mixed with 5 mM EDTA and 4 mM sodium metabisulphite for preservation of catecholamines and stored at −80 °C. Control experiments showed that all detectable adrenaline was degraded after incubation in medium for 24 h at 37 °C. Thus, any adrenaline identified in the medium must have been secreted by cells in the last 24 h before collecting the medium.

Human U937 cells were cultured in RPMI 1640 medium with 5% FBS and antibiotics, and were differentiated to M1 macrophage-like cells by incubating with 20 nM phorbol 12-myristate 13-acetate (PMA, Sigma) for 24 h and further culturing in RPMI 1640 medium with 5% FBS and antibiotics for another 72 h. The experiments with U937 were set up in the same way as described above with peritoneal macrophages. Ten minutes before the addition

Author Manuscript Author Manuscript Author Manuscript Author Manuscript

of LPS or adrenaline, MTR at 2 mM or ANP at 5 μg ml^{-1} was added to the cells. Cells were incubated for 24 h with LPS at 1 μg ml^{-1}.

LPS experiments in mice.

LPS from *Escherichia coli* 0111:B4 was formulated as a 10 mg ml^{-1} solution in water and stored in −80 °C. In BALB/C mice, LPS was injected intraperitoneally at a lethal dose of 3.5 mg kg^{-1}. This lethal dose was found to cause 70–90% death rate and be optimal for demonstrating the protective effects of ANP and MTR. In experiments with catecholamine pumps that were implanted a day before, a sublethal dose of LPS with 15–35% death rate was optimized in BALB/C mice. In $Th^{+/+}$ and $Th^{\Delta LysM}$ mice with C57Bl/6 background, a lethal dose of LPS was optimized at 5 mg kg^{-1}. Human ANP (Sigma) was dissolved in saline, loaded in mini-osmotic pumps (ALZET) with a release rate of 12 μg per day and implanted subcutaneously in the back of mice 12 h before the LPS injection. Mice implanted with pumps loaded with saline served as controls. MTR was freshly dissolved in PBS and injected intraperitoneally at the indicated doses for three days before the LPS treatment. One hour before the LPS injection, MTR was injected into the lower abdomen contralateral to the side of LPS injection. The control groups were injected with PBS. For the following 3 days, MTR was injected intraperitoneally at reduced indicated doses. Hydration of mice was supported by daily subcutaneous injection of 0.5 ml saline.

CLP experiments.

CLP was performed as described previously[32]. Briefly, 6–8-week-old female C57Bl/6 mice were anesthetized and following abdominal incision, the caecum was ligated at about a quarter of the distance from the luminal entry to its tip. The ligated caecum was punctured through and through with a 22G needle at one half and three quarters of the distance from the luminal entry to its tip. A small amount of the caecal content was gently pushed out of the four openings into the peritoneum. Subsequently, the abdominal muscles were sutured and the skin was closed with two staples. Immediately after this, 500 ml of saline was injected subcutaneously to the mice. For the groups treated with antibiotics, imipenem (Sigma) was injected subcutaneously at 25 mg kg^{-1} starting from 20 h after CLP, with a schedule of twice a day on day one and once a day thereafter for 10 days. MTR was freshly dissolved in PBS and injected intraperitoneally at 60 mg kg^{-1} per day for three days before the CLP. Twenty minutes before the CLP, MTR was injected at 60 mg kg^{-1} intraperitoneally into the right side. The control groups were injected with PBS. For the following 4 days, MTR was injected at 30 mg kg^{-1} per day intraperitoneally into the right side. Hydration of mice was supported by daily subcutaneous injection of 0.5 ml saline.

Anti-CD3 treatment.

For survival experiments, 5–6-month-old female BALB/c mice were used because we observed that young mice treated with anti-CD3 antibodies underwent severe weight loss but did not consistently die, even at very high doses of the anti-CD3 antibody. MTR was freshly dissolved in PBS and injected intraperitoneally at 60 mg kg^{-1} per day for three days before injection of anti-CD3 antibodies. Various doses of anti-CD3 antibody were tested, and it was found that 125 μg per mouse resulted in the death of about half the mice; this was the dose chosen for further experiments. Thirty minutes before the intraperitoneal injection of the

Author Manuscript Author Manuscript Author Manuscript Author Manuscript

anti-mouse CD3 antibody (BioXcell, 145–2C11), MTR was intraperitoneally injected at 60 mg kg^{-1} into the contralateral side. A single additional dose of 30 mg kg^{-1} MTR was injected intraperitoneally on the following day. Control groups were injected with PBS at the same times. For experiments with conditional TH-knockout mice, 4–6-week-old $LysM^{cre}$ $Th^{fl/fl}$ ($Th^{\Delta LysM}$) mice with C57Bl/6 background were used and $LysM^{cre}$ $Th^{+/+}$ mice of the same age were used as control. In these experiments, 200 μg per mouse anti-mouse CD3 antibody was injected intraperitoneally.

Human anti-CD19 CART (hCART19) cells and untransduced T cells (UT-T).

Human CD19scFv-CD28–4–1BB-CD3ζ CAR-T cells (PM-CAR1003) were purchased from Promab Biotechnologies and stored in liquid nitrogen upon delivery. The CAR construct includes a scFv derived fromFMC63 anti-CD19 antibody, a hinge region and a transmembrane domain of CD28 in a third-generation CAR cassette. Generation of CAR-encoding lentivirus, isolation, expansion and transduction of human T cells followed the procedures published before by the manufacturer[33]. Cells were proliferated for two weeks in medium containing 300 IU ml^{-1} of human IL-2 by the manufacturer[33]. CART cells were used freshly upon defrosting or maintained less than 7 days in the CART medium consisting of AIM-V medium (GIBCO) supplemented with 5% FBS (Sigma) and penicillin-streptomycin (GIBCO), with the addition of 300 IU ml^{-1} of human IL-2 (Peprotech).

UT-T were purchased from ASTARTE Biologics (1017–3708OC17, $CD3^+$) and were used freshly upon defrosting or maintained less than 7 days in CART medium.

In vitro assays of hCART19 cells.

Raji, a human Burkitt's lymphoma cell line, was purchased from Sigma. In a 48-well plate, Raji cells were plated at 1×10^5 per well and hCART19 cells or UT-T cells were plated at 5×10^5 per well in 275 μl of medium. A solution of 3 mg ml^{-1} (−)-adrenaline was made in 0.1N HCl and subsequently diluted in PBS for use at a final concentration of 15 ng ml^{-1}. Five minutes before the Raji and CART cells with or without adrenaline were mixed, MTR at 2 mM or human ANP at 5 μg $ml^{-1}$was added and then the cells were incubated for 24 h at 37 °C. Control experiments showed that all detectable adrenaline was degraded after incubation in medium for 24 h at 37 °C. Thus, any adrenaline identified in the medium must have been secreted by cells in the last 24 h before collecting the medium. Cycloheximide (CHX, Sigma) was added at 10 μg ml^{-1} to Raji and CART cells 30 min before they were mixed. After incubation, the cells were pelleted by centrifugation at 700*g* and 4 °C for 5 min and the supernatants were collected and mixed with 5 mM EDTA and 4 mM sodium metabisulphite for preservation of catecholamines, then stored at −80 °C until analysis.

Treatment of Raji tumour-bearing mice with hCART19 cells.

We purchased 6–8-week-old female NSG-SGM3 (NSGS) mice (NOD.Cg-$Prkdc^{scid}$ $Il2rg^{tm1Wjl}$Tg (CMV-IL3, CSF2, KITLG) 1Eav/MloySzJ, stock number 013062) from the Jackson Laboratory. Raji cells were transfected with a luciferase construct via lentivirus to create Raji–luc cells. NSGS is a triple transgenic strain expressing human IL3, GM-CSF and SCF combining the features of the highly immunodeficient NOD scid gamma (NSG) mouse. One day before the injection of Raji cells, mice were irradiated at a dose of 2 Gy in a CIXD

Author Manuscript Author Manuscript Author Manuscript Author Manuscript

Xstahl device. In high tumour burden experiments in Fig. 4, 10^6 Raji–luc cells were injected intravenously through the tail vein. Six days later, tumour loads were assessed using a Xenogen instrument and 15×10^6 hCART19 cells or UT-T were injected intravenously. In low tumour burden experiments in Figs. 5, 2×10^5 Raji–luc cells were injected intravenously through the tail vein. Four days later, tumour loads were assessed using a Xenogen instrument and 15×10^6 hCART19 cells were injected intravenously. MTR was injected intraperitoneally at 60 mg kg^{-1} per day for 3 days before the hCART19 injection. On the day of CART19 injection, a fourth dose of 60 mg kg^{-1} was given intraperitoneally and the mice were subsequently injected four more times at daily intervals at 30 mg kg^{-1}.

Mouse anti-CD19 CART cells (mCART19) and untransduced T cells (UT-T).

Mouse CD19scFv-CD28-CD3ζ CAR (m1928z) construct with GFP in SFG retroviral vector was described before and provided by M. Davila at the Moffitt Cancer Center[34]. The isolation, activation and transduction of mouse T cells followed the procedure described before[34,35]. Briefly, the spleens were collected from female C57Bl/6 mice and T cells were enriched from splenocytes by passage over a nylon wool column (Polysciences). Mouse T cells were then activated with CD3/CD28 Dynabeads (Thermo Fisher) following the manufacturer's instructions and cultured in the presence of human IL-2 at 30 IU ml^{-1} (R&D Systems). Retrovirus was produced by transfecting Phoenix-Eco packaging cells (ATCC) and spinoculations were done twice with retroviral supernatant. mCART19 cells were expanded for 10–14 days as described[35]. UT-T were produced following the same procedure without viral transduction.

Treating B cell acute lymphoblastic leukaemia (B-ALL) with mCART19 in immunocompetent mice.

The Eμ-ALL cell line was derived from a lymphoid malignancy in an Eμ-myc transgenic mouse and upon intravenous injection, can develop B-ALL in C57Bl/6 mice[34]. The Eμ-ALL cells were provided by M. Davila and co-cultured with feeder NIH-3T3 cells that were irradiated at 60 Gy, in RPMI 1640 medium supplemented with 10% FBS, 0.05 mM 2-mercaptoethanol and antibiotics. Eμ-ALL cells were transfected with luciferase via lentivirus. 2×10^6 Eμ-ALL cells were intravenously injected in female 6–8-week-old C57Bl/6 mice through the tail vein and after 6 days, mice were intraperitoneally injected with cyclophosphamide (CPA) at 100 mg kg^{-1} for pre-conditioning as described before[34]. One day after CPA treatment, 10×10^6 mCART19 cells were intravenously injected in the mice. MTR was injected intraperitoneally at 40 mg kg^{-1} per day for 3 days before the mCART19 injection. On the day of mCART19 injection, a fourth dose of 40 mg kg^{-1} was given intraperitoneally and the mice were subsequently injected four more times at daily intervals at 30 mg kg^{-1}. One day before mCART19 injection, mini-osmotic pumps (ALZET) loaded with human ANP with a release rate of 12 μg per day were implanted subcutaneously in the back of mice. Tumour load was monitored by Xenogen before and after mCART19 injection.

Measurement of catecholamines and cytokines in mouse plasma.

Blood samples were collected into tubes containing 5 mM EDTA and 4 mM sodium metabisulphite after puncturing the facial vein or (terminally) by cardiac puncture.

Author Manuscript Author Manuscript Author Manuscript Author Manuscript

Subsequently, the samples were centrifuged and the plasmas were stored at −80 °C before analysis. Catecholamines (dopamine, noradrenaline and adrenaline) were measured using the 3-CAT Research ELISA kit from Labor Diagnostika Nord GmbH/Rocky Mountain Diagnostics. Cytokines were measured using Luminex assays based on Millipore Mouse and Human Cytokine/Chemokine panels or ELISA kits for mouse or human IL-6, TNF, MIP-1α, KC, MIP-2 and IL-2 (R&D Systems) per manufacturer's instructions.

Statistical analysis.

Statistical analysis was performed using GraphPad Prism 7 and R version 3.5.1. Statistical tests performed by Graphpad Prism included the two-tailed unpaired two-sample *t*-test; one-tailed unpaired two-sample *t*-test; the log-rank Mantel–Cox test; the Gehan–Breslow–Wilcoxon test; the weighted log-rank test using Fleming–Harrington weights was performed in R. The respective statistical test used for each figure is noted in the corresponding figure legends and significant statistical differences are noted as $*P \leq 0.05$, $**P \leq 0.01$, $***P \leq 0.001$, **** $P \leq 0.0001$.

Reporting summary.

Further information on research design is available in the Nature Research Reporting Summary linked to this paper.

Extended Data

Author Manuscript Author Manuscript Author Manuscript Author Manuscript

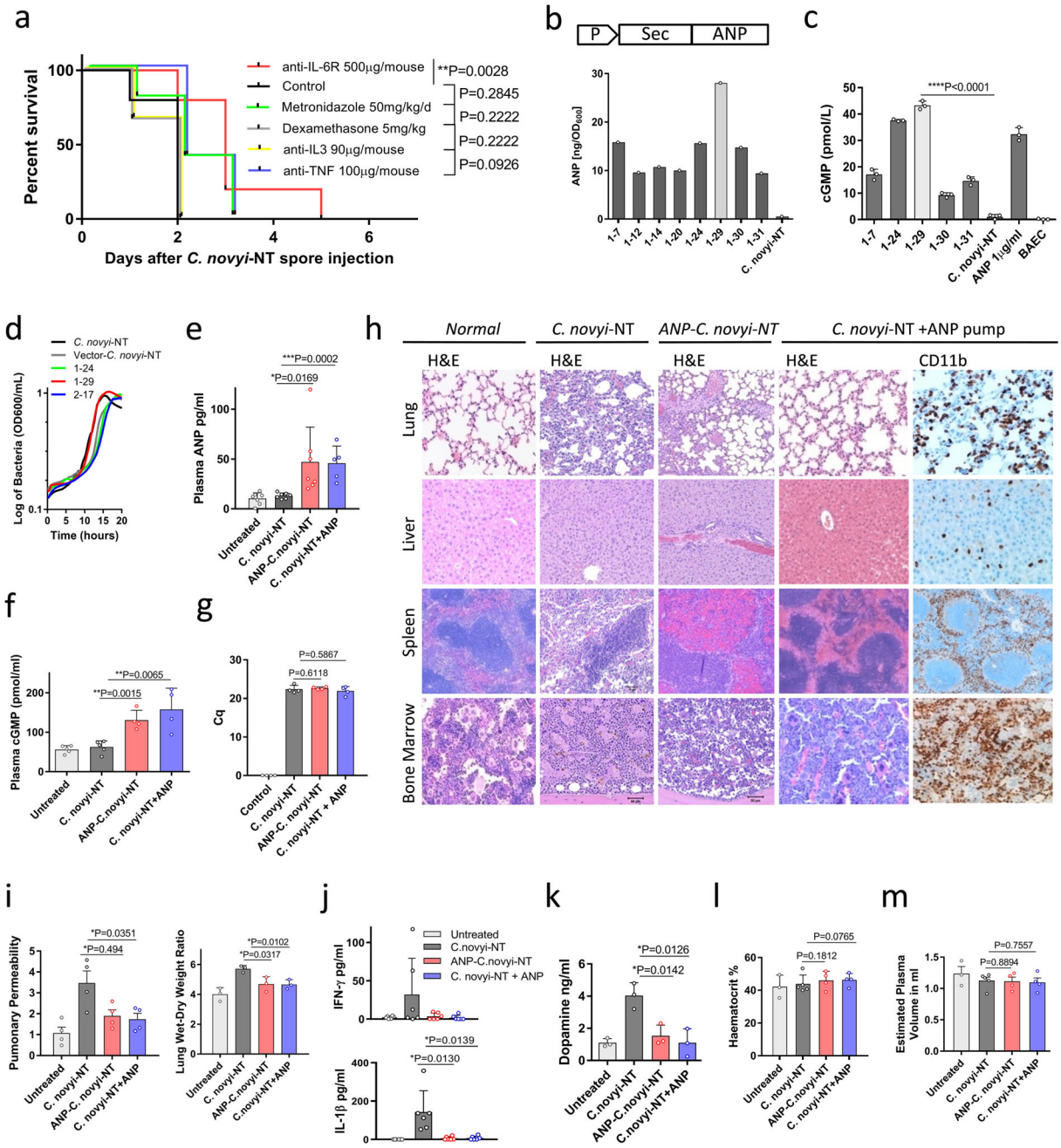

Extended Data Fig. 1 |. In vitro and in vivo studies of ANP-*C. novyi*-NT.

a, Kaplan–Meier curves of mice with large subcutaneous CT26 tumours (600–900 mm^3), treated with 12×10^6 *C. novyi*-NT spores and the indicated agents: anti-IL-6R ($n = 10$), metronidazole ($n = 5$), dexamethasone ($n = 6$), anti-IL3 ($n = 6$) and anti-TNF ($n = 5$) injected intratumourally, compared to controls ($n = 5$). Survival differences were analysed by two-sided log-rank test. **b** and **c**, Selected clones of ANP-*C. novyi*-NT were analysed for ANP secretion, shown as the average of a triplicate, (**b**) and for cGMP induction ($n = 3$) using bovine aortic endothelial cells (**c**). **d**, Growth pattern of several clones compared to the parental *C. novyi*-NT. The average of a triplicate is shown. **e**–**g**, Levels of plasma ANP (left

Author Manuscript Author Manuscript Author Manuscript Author Manuscript

to right, n = 7, 8, 7, 5 independent samples per column) (**e**), plasma cGMP (n = 5, 5, 4, 4 samples per column) (**f**) and germinated *C. novyi* strains in tumour tissue (n = 4 samples per column) based on quantification cycle (C_q) from RT–PCR of germination-specific NT01CX1854 gene (**g**), measured at 36 h after spore injection. **h**, Representative haematoxylin and eosin as well as anti-CD11b antibody stained sections from the lungs, liver, spleen and bone marrow of mice treated with *ANP-C. novyi*-NT (n = 3), *C. novyi*-NT (n = 3) and *C. novyi*-NT plus ANP (n = 2) compared to normal controls (n = 2). **i**–**m**, Pulmonary permeability (n = 4 mice per group), lung wet–dry ratio (n = 3 mice per group) (**i**) as well as levels of cytokines (n = 6 independent samples per column) (**j**), dopamine (n = 3 independent samples per column) (**k**), haematocrit (n = 3, 5, 4, 4 samples per column) (**l**) and calculated plasma volume (n = 3, 5, 4, 4 samples per column) (**m**) measured 36 h after spore treatment. Data are presented as mean ± s.d. with individual data points shown, analysed by two-tailed *t*-test (**c**, **e**–**g**, **i**–**m**). BAEC, bovine aortic endothelial cells.

Author Manuscript Author Manuscript Author Manuscript Author Manuscript

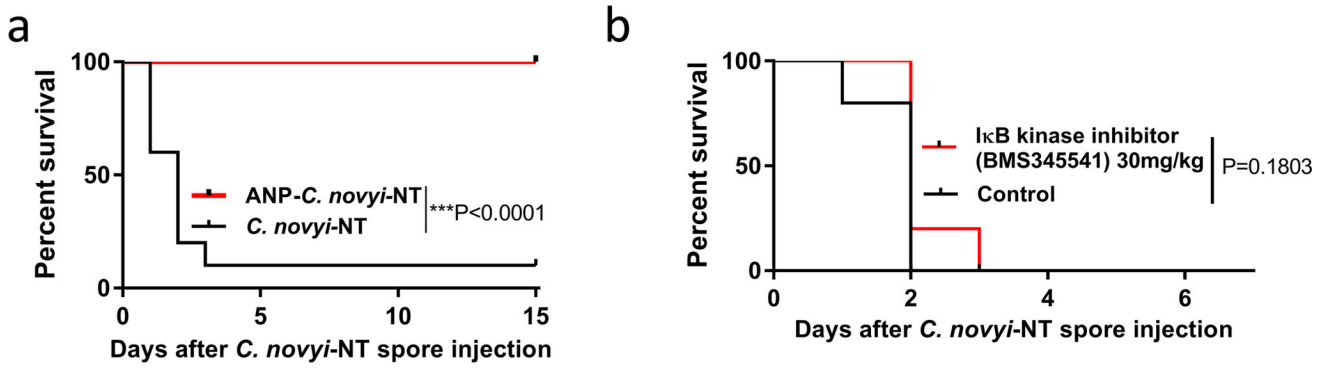

Extended Data Fig. 2 |. Survival of mice treated with ANP and IκB kinase inhibitor BMS345541.
a, Survival of mice with subcutaneously implanted GL-261 tumours, treated with 12×10^6 of ANP-*C. novyi*-NT spores ($n = 10$ animals per group). **b**, Survival of mice with CT26 tumours treated with *C. novyi*-NT and IκB kinase inhibitor BMS345541 ($n = 5$ mice per group). Survival differences were analysed by two-sided log-rank test (**b**, **c**).

Author Manuscript
Author Manuscript
Author Manuscript
Author Manuscript

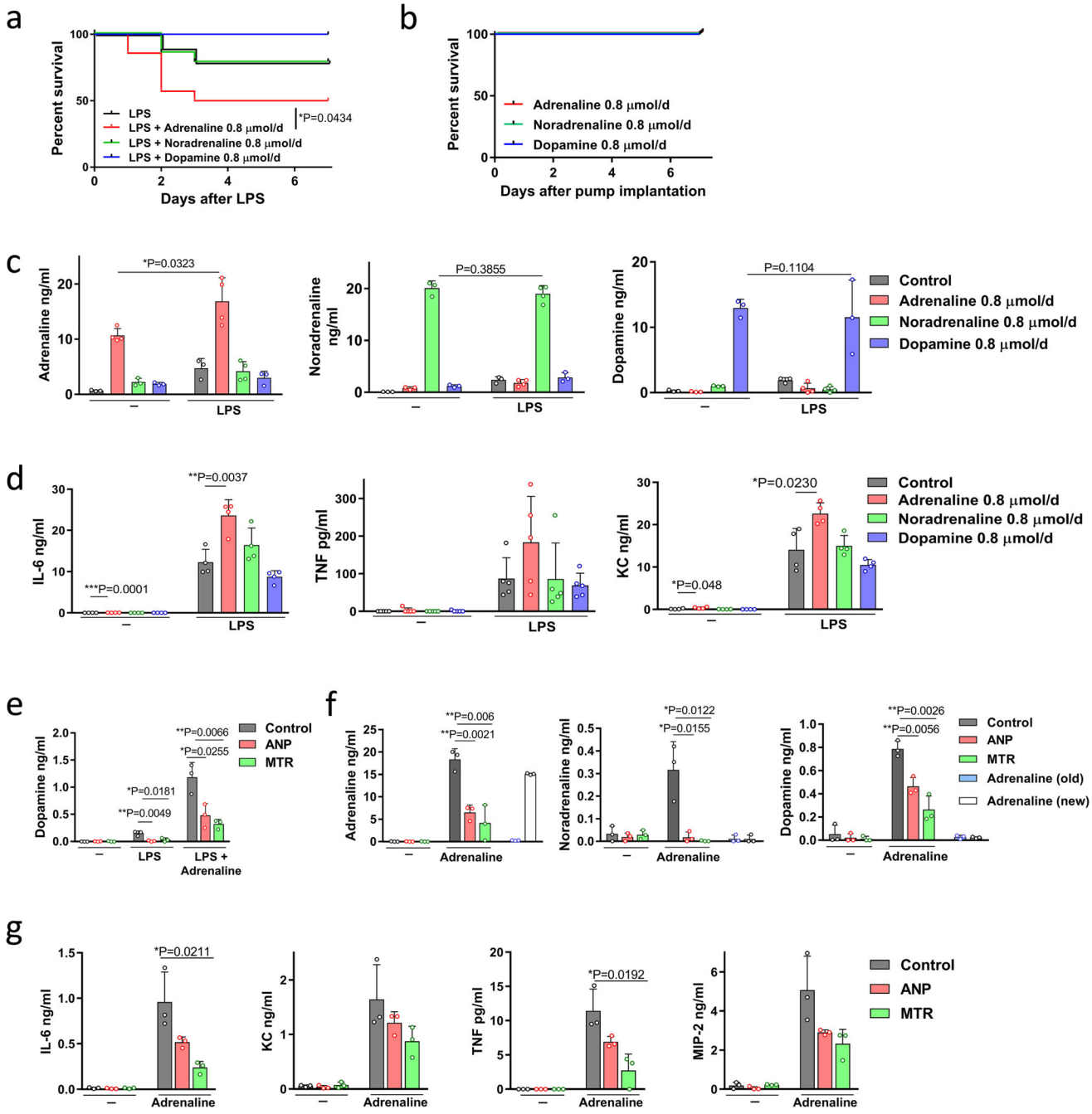

Extended Data Fig. 3 |. Adrenaline enhances the inflammatory response.

a, Survival of BALB/c mice implanted with the indicated catecholamine pump and stimulated with a sublethal dose of LPS (n = 14 mice per group) compared to LPS alone (n = 19 mice). Survival differences were analysed by Gehan–Breslow–Wilcoxon test. **b**, Survival of BALB/c mice with indicated catecholamine pump without LPS stimulation (n = 5 mice per group). **c**, **d**, 24 h plasma levels of adrenaline (left to right, n = 3, 4, 3, 3, 3, 4, 4, 3 per column), noradrenaline (n = 3, 3, 3, 3, 3, 4, 4, 3) and dopamine (n = 3, 3, 3, 3, 3, 4, 4, 3) (**c**) as well as levels of IL-6 (n = 4 per column), TNF (n = 5 per column) and KC (n = 4 per column) (**d**) in mice receiving the indicated treatments. **e**, Dopamine concentration in LPS-

Author Manuscript Author Manuscript Author Manuscript Author Manuscript

and adrenaline-treated peritoneal macrophages pre-incubated with ANP or MTR ($n = 3$ per column), measured after 24 h. **f**, **g**, Levels of catecholamines ($n = 3$ independent samples per column) (**f**) and several cytokines ($n = 3$ independent samples per column) (**g**) in adrenaline (15 ng ml^{-1})-treated peritoneal macrophages pre-incubated with ANP or MTR and measured after 24 h. Data are presented as mean ± s.d. with individual data points shown, analysed by two-tailed *t*-test (**c**–**g**).

Author Manuscript Author Manuscript Author Manuscript Author Manuscript

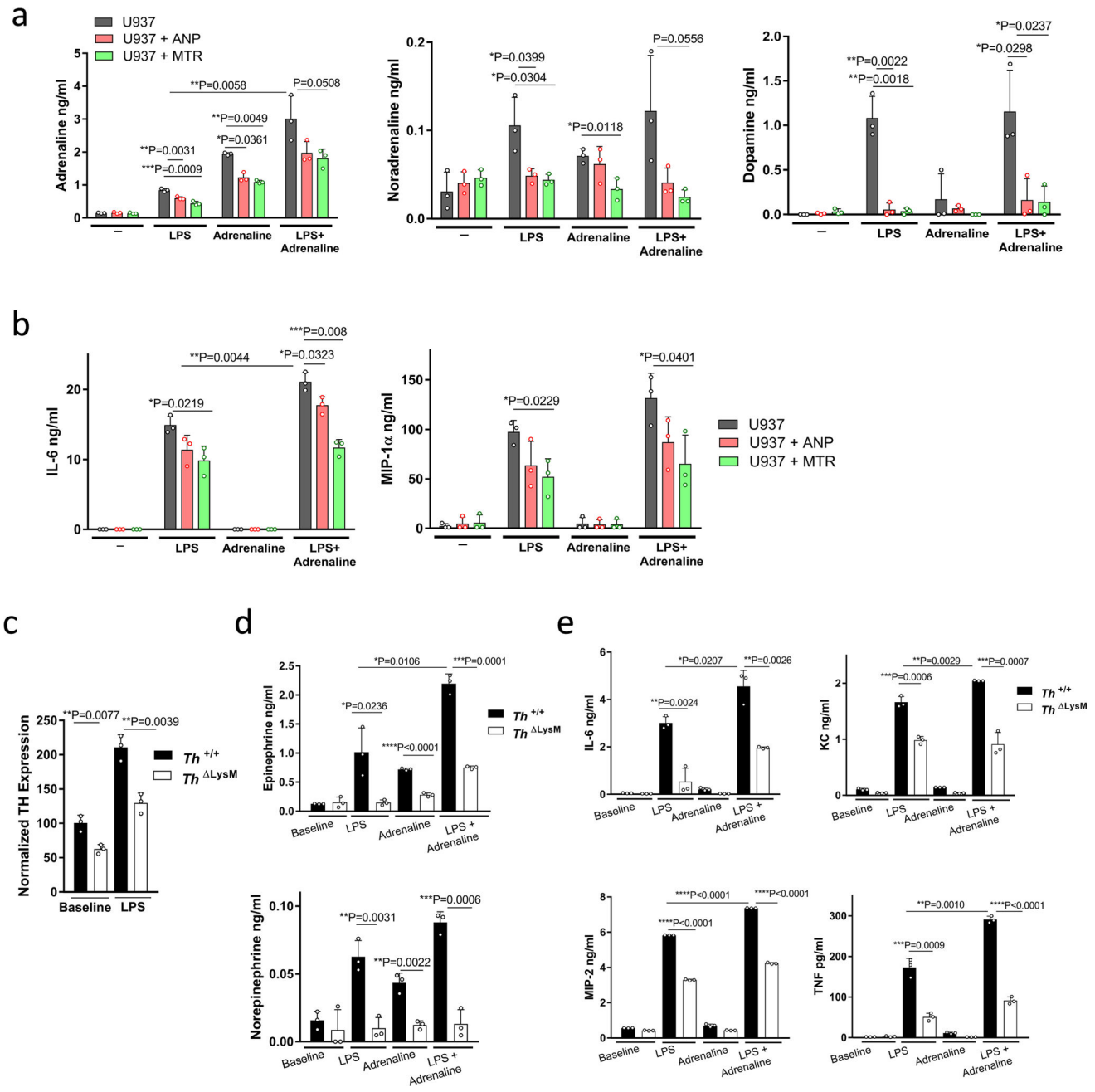

Extended Data Fig. 4 |. Catecholamines modulate the cytokine release in macrophages in vitro. **a**, **b**, Human U937 macrophage-like cells were pre-treated with ANP or MTR for 10 min, then stimulated with LPS at 1 μg ml^{-1} and/or adrenaline at 15 ng ml^{-1}. Culture supernatants were analysed for catecholamines (n = 3 per column) (**a**) as well as the indicated cytokines (n = 3 per column) (**b**). **c**, *TH* expression of baseline and LPS-stimulated $Th^{+/+}$ or $Th^{\Delta LysM}$ macrophages (n = 3 per group), analysed by RT–PCR; results are normalized to ubiquitin C (*UBC*) expression. **d**, **e**, Supernatants of collected peritoneal macrophages from $Th^{+/+}$ or $Th^{\Delta LysM}$ mice, stimulated with LPS at 50 μg ml^{-1}, adrenaline 15 μg ml^{-1} or both for 24 h, were analysed for levels of adrenaline (n = 3), noradrenaline (n = 3) (**d**) and cytokines IL-6

Author Manuscript Author Manuscript Author Manuscript Author Manuscript

($n = 3$), KC ($n = 3$), MIP-2 ($n = 3$) and TNF ($n = 3$) (**e**). All data are presented as mean ± s.d. with individual data points shown, analysed by two-tailed *t*-test.

Author Manuscript Author Manuscript Author Manuscript Author Manuscript

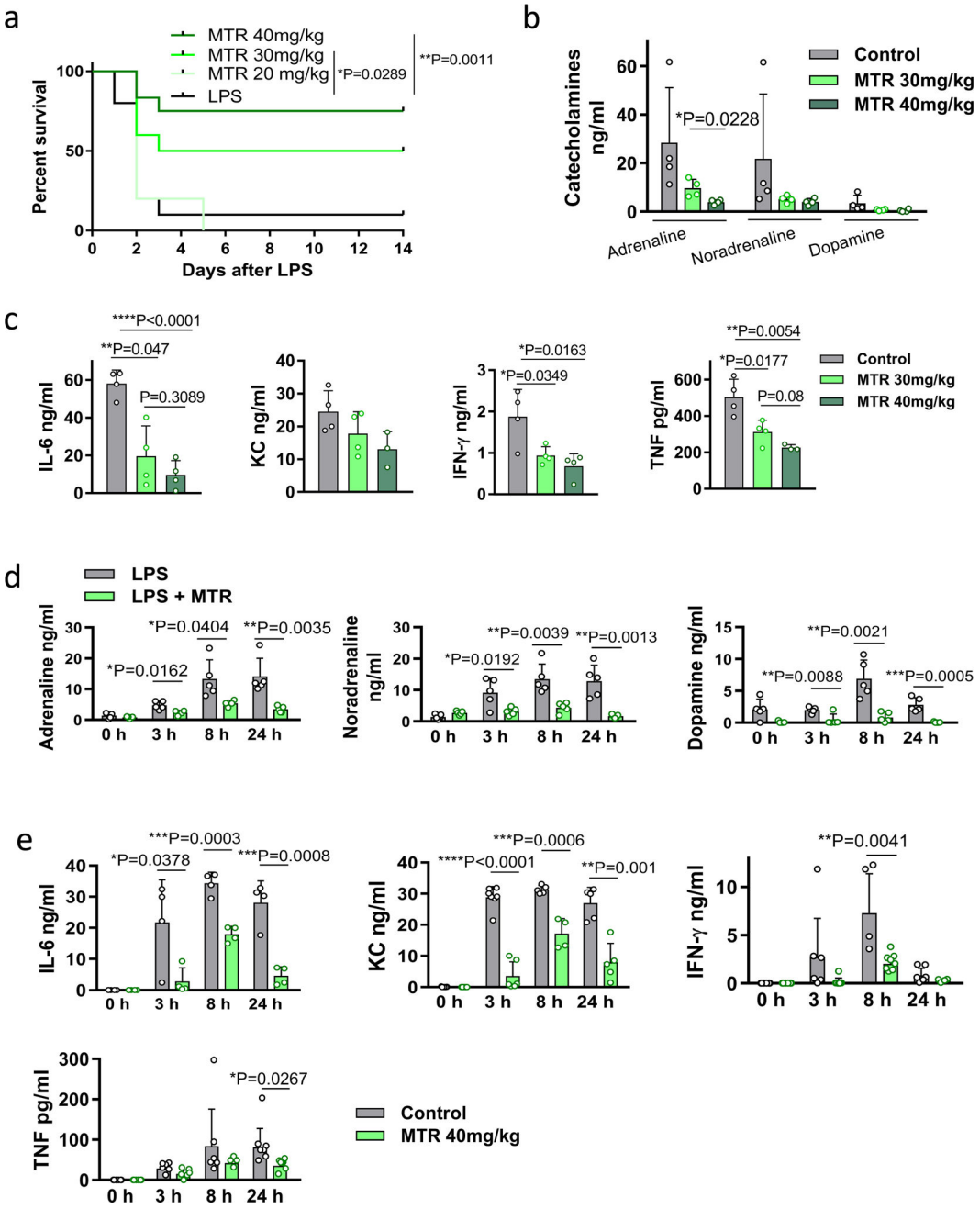

Extended Data Fig. 5 |. Modulation of catecholamine synthesis by MTR dose-dependently determines survival and cytokine release.

a, Survival of BALB/c mice stimulated with a lethal dose of LPS and treated with the indicated dose of MTR: MTR 20 mg kg^{-1} (n = 5 mice per group); MTR 30 mg kg^{-1} (n = 10 mice), MTR 40 mg kg^{-1} (n = 12) compared to LPS (n = 10 mice). Survival differences were analysed by two-sided log-rank test. **b**, **c**, Levels of plasma catecholamines (n = 4 per column) (**b**) and IL-6 (n = 4 per column), KC (left to right, n = 4, 4, 3 per column), IFN-γ (n = 4) and TNF (n = 4, 4, 3) (**c**) at different MTR doses measured 24 h after LPS injection. **d**, **e**, 24-h-time course of circulating adrenaline (n = 5, 5, 5, 4, 5, 4, 5, 5), noradrenaline (n =

Author Manuscript Author Manuscript Author Manuscript Author Manuscript

5) and dopamine (n = 5) (**d**) and corresponding levels of IL-6 (n = 4), KC (n = 7, 7, 7, 6, 5, 4, 5, 5), IFN-γ (n = 6, 6, 6, 8, 4, 8, 6, 4) and TNF (n = 6, 6, 6, 6, 6, 4, 7, 7) (**e**) in LPS-treated mice receiving MTR 40 mg kg^{-1}. Data are presented as mean ± s.d. with individual data points shown, analysed by two-tailed t-test (**b**–**e**).

Author Manuscript Author Manuscript Author Manuscript Author Manuscript

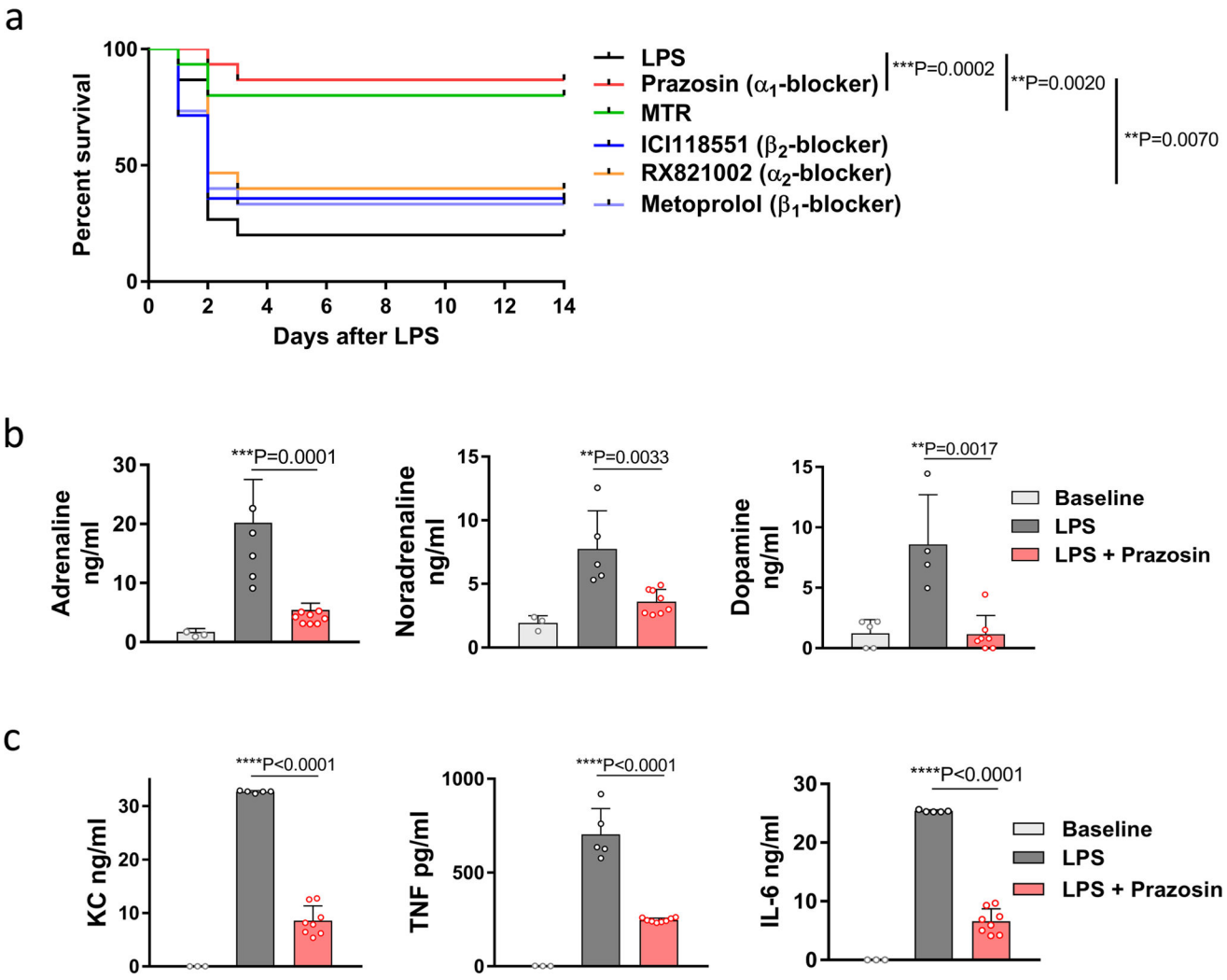

Extended Data Fig. 6 |. Blockage of α_1-adrenoceptor mediates the survival in experimental systemic inflammatory syndrome.

a, Kaplan–Meier curve of LPS-injected BALB/c mice treated with the indicated adrenoreceptor blockers (n = 15 animals per group). Survival differences were analysed by two-sided log-rank test. **b**, **c**, Levels of adrenaline, noradrenaline (left to right, n = 3, 5, 8 per column) and dopamine (n = 5, 4, 7) (**b**) as well as indicated cytokines (n = 3, 5, 8) (**c**) measured 24 h after LPS administration. Data are presented as mean ± s.d. with individual data points shown, analysed by two-tailed t-test (**b**, **c**).

Author Manuscript Author Manuscript Author Manuscript Author Manuscript

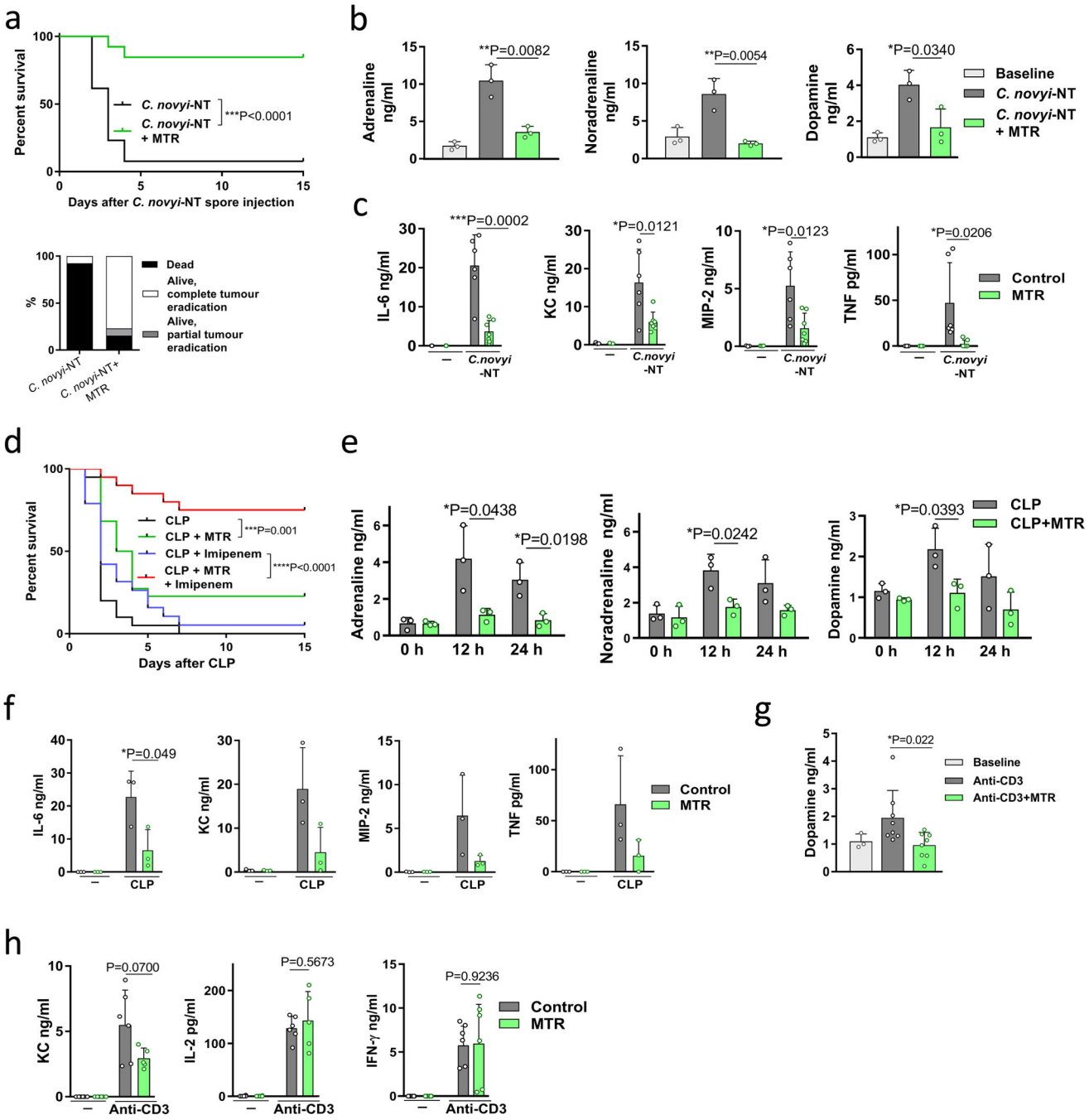

Extended Data Fig. 7 |. Suppression of catecholamines with MTR reduces toxicity of oncolytic bacterium *C. novyi*-NT and polymicrobial sepsis.

a, Survival (top panel) and therapeutic response (bottom panel) of CT26 tumour-bearing BALB/c mice undergoing *C. novyi*-NT treatment with or without MTR pre-treatment (n = 13 mice per group). Survival differences were analysed with two-sided log-rank test. **b**, **c**, Corresponding plasma levels of adrenaline (n = 3 independent samples per column), noradrenaline (n = 3), dopamine (n = 3) (**b**) and indicated cytokines (left to right, n = 3, 3, 6, 7 independent samples per column) (**c**), measured at baseline and 36 h after treatment. **d**, Survival of C57Bl/6 mice undergoing CLP, with the indicated treatments (CLP, n = 20 mice;

Author Manuscript Author Manuscript Author Manuscript Author Manuscript

MTR, $n = 22$; imipenem, $n = 19$; MTR + imipenem, $n = 20$ mice per group). Survival differences were analysed with two-sided log-rank test. **e**, Plasma levels of adrenaline ($n = 3$), noradrenaline ($n = 3$) and dopamine ($n = 3$) at the indicated time points after CLP, with or without MTR pre-treatment. **f**, Levels of indicated cytokines ($n = 3$) at baseline and 24 h after CLP, with or without MTR pre-treatment. **g**, **h**, Levels of plasma dopamine (left to right, $n = 3, 8, 8$ independent samples per column) (**g**) and KC ($n = 6, 6, 6, 5$), IL-2 ($n = 6, 6, 6, 5$) and IFN-γ ($n = 6$) (**h**) measured 24 h after α-CD3 treatment, with or without MTR. Data are presented as mean ± s.d. with individual data points shown, analysed by two-tailed *t*-test (**b**, **c**, **e**–**h**).

Author Manuscript Author Manuscript Author Manuscript Author Manuscript

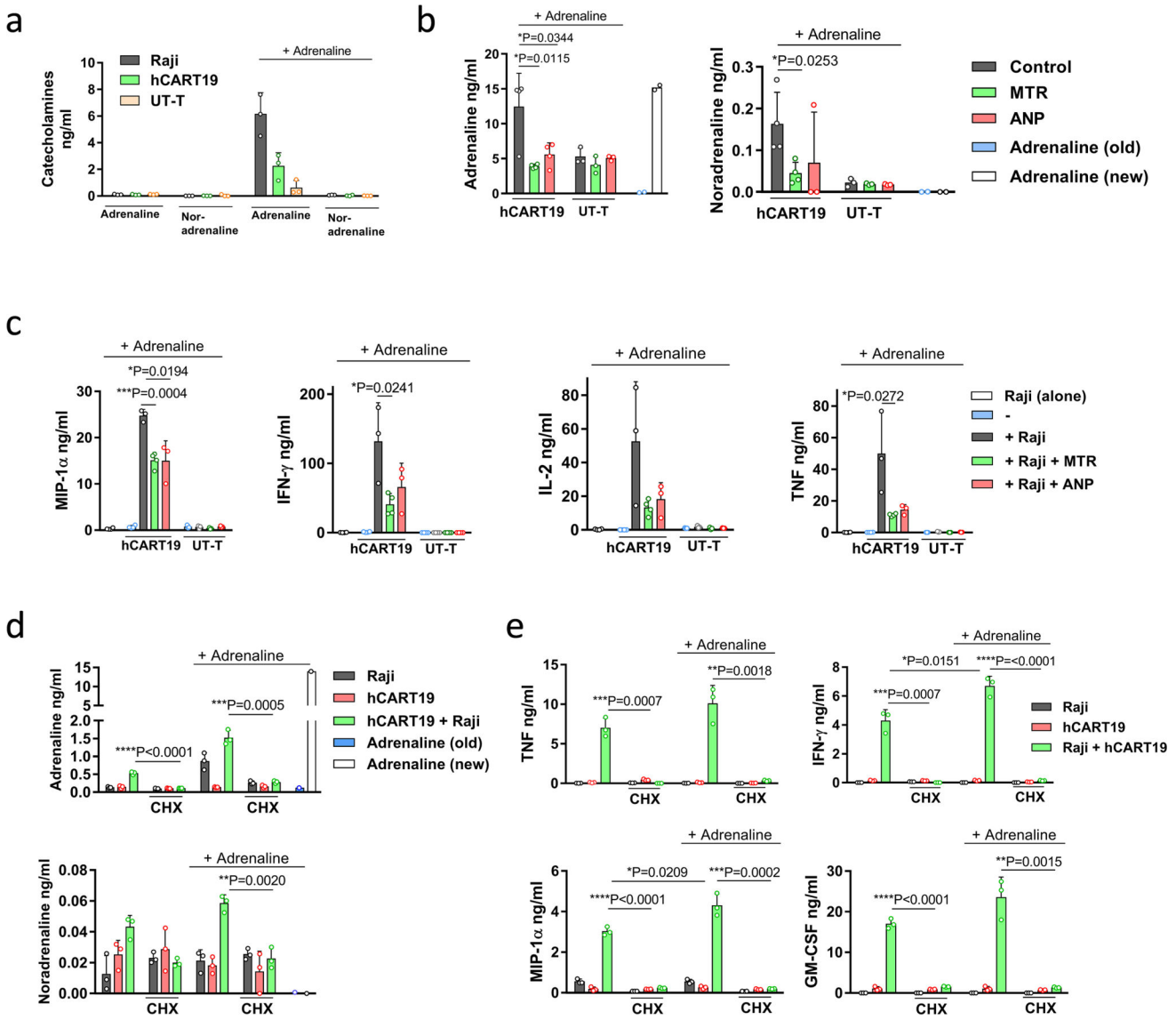

Extended Data Fig. 8 |. Adrenaline stimulates cytokine release during hCART19–Raji cell interaction in vitro.

a, Levels of catecholamines measured individually in supernatants of Raji cells (n = 3), hCART19 (n = 3) and UT-T (n = 3 per column) at baseline and when exposed to adrenaline. **b**, **c**, Co-cultures of hCART19 and Raji with or without MTR or ANP pre-treatment were stimulated with 15 ng ml^{-1} of adrenaline. Culture supernatants were collected after 24 h and analysed for adrenaline (left to right, n = 4, 4, 4, 3, 3, 3, 2, 2 per column) and noradrenaline (n = 4, 4, 3, 3, 3, 3, 2, 2). Adrenaline (old): adrenaline at 15 ng ml^{-1} was incubated at 37 °C for 24 h in the cell-free medium. Adrenaline (new): adrenaline at 15 ng ml^{-1} was added into the cell-free medium and immediately measured (**b**). Corresponding cytokine levels of MIP-1α (n = 4, 4, 3, 4, 3, 3, 3, 3, 3), IFN-γ (n = 4, 4, 3, 4, 3, 4, 4, 4, 4), IL-2 (n = 4, 4, 3, 4, 3, 3, 3, 3, 3) and TNF (n = 4, 4, 3, 4, 3, 3, 3, 3, 3) (**c**). UT-T served as control. **d**, **e**, As above, co-cultures of hCART19 and Raji with or without CHX were stimulated with 15 ng ml^{-1} of adrenaline in vitro. Levels of catecholamines (n = 3, 3, 3, 3, 3, 3, 3, 3, 3, 3, 3, 3, 1, 1) (**d**) and

indicated human cytokines ($n = 3$) (**e**) were measured after 24 h. Data are presented as mean ± s.d. with individual data points shown, analysed by two-tailed *t*-test.

Author Manuscript Author Manuscript Author Manuscript Author Manuscript

Author Manuscript Author Manuscript Author Manuscript Author Manuscript

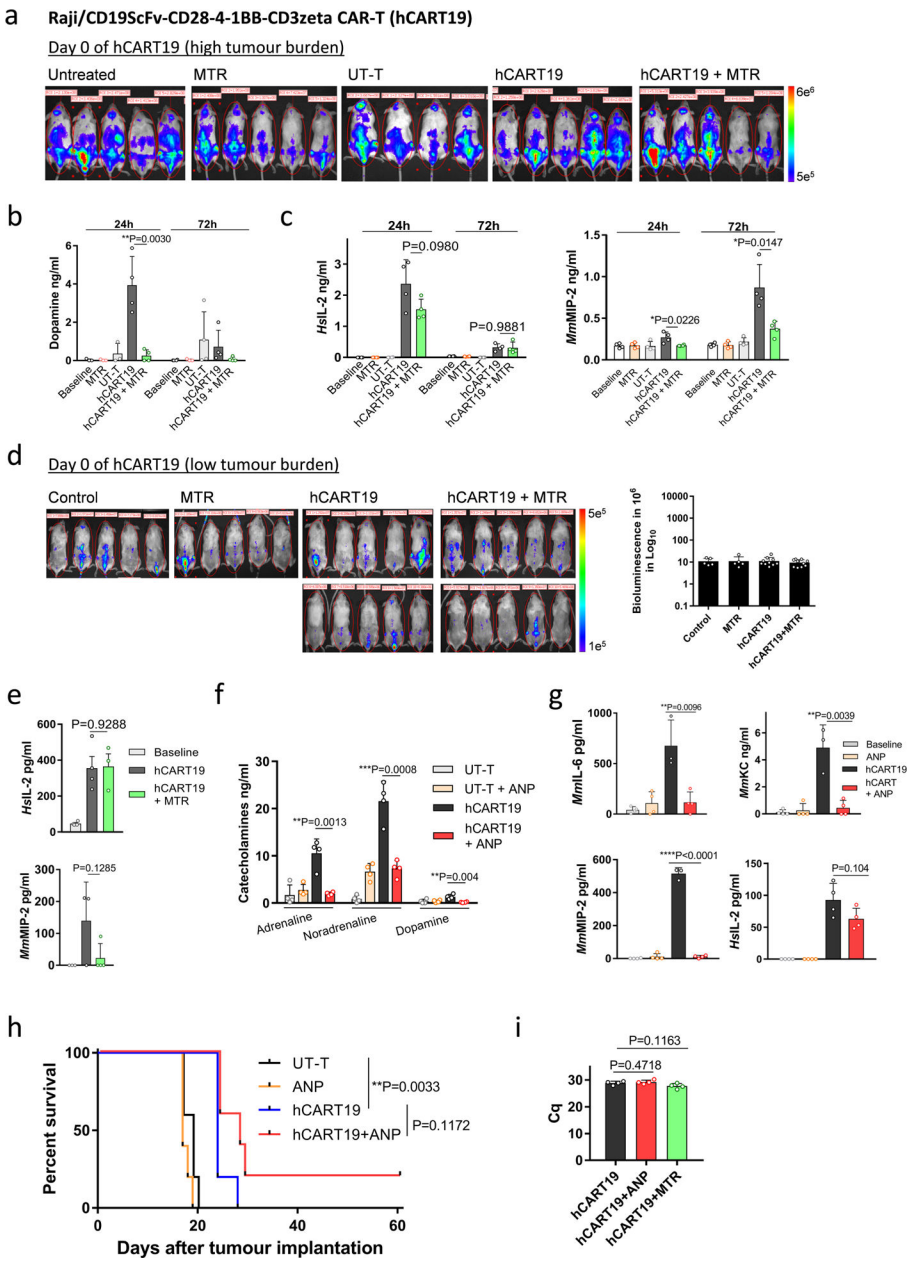

Extended Data Fig. 9 |. MTR and ANP prevent cytokine release in Raji/hCART19 mouse model. **a**, Bioluminescent images (BLI) of Raji-bearing NSGS mice with high tumour burden. At day 0, tumour engraftment was quantified by BLI and mice were assigned to the treatment groups (untreated, MTR, hCART19, hCART19+MTR, $n = 5$ mice per group; UT-T, $n = 4$). **b**, **c**, Levels of dopamine (left to right, $n = 3, 3, 3, 4, 4, 4, 3, 4, 4, 4$ per column) (**b**) and indicated cytokines ($n = 4$) (**c**) measured in mice (with high tumour burden) 24 and 72 h after hCART19 and UT-T injection. **d**, BLI of Raji-bearing NSGS mice with low tumour burden. At day 0, mice were randomly assigned based on tumour burden to receive hCART19, with or without MTR ($n = 10$ mice per group) or UT-T, with or without MTR ($n = 5$ mice per group). **e**, Levels of *Hs*IL-2 ($n = 4, 4, 3$) and *Mm*MIP-2 ($n = 3, 3, 4$) assessed 72 h after hCART19 injection in mice with low tumour burden. **f**, **g**, NSGS mice were

Author Manuscript Author Manuscript Author Manuscript Author Manuscript

injected with hCART19 4 days after Raji implantation and treated with ANP delivered via subcutaneously implanted osmotic pumps. Levels of circulating catecholamines ($n = 4$ per column) (**f**) and *Mm*IL-6, *Mm*KC and *Mm*MIP-2 ($n = 4, 4, 3, 4$) as well as *Hs*IL-2 ($n = 4$) (**g**) were assessed 24 h after hCART19 administration. **h**, Survival of Raji cell-bearing NSGS mice treated with hCART19 and ANP ($n = 5$ per group); analysed by two-sided log-rank test. **i**, Level of circulating hCART19 10 days after treatment, determined by C_q from RT–PCR and analysed in triplicates ($n = 4$ per group). Data are presented as mean ± s.d. with individual data points shown, analysed by two-tailed *t*-test (**b**, **c**, **e**–**i**).

Author Manuscript Author Manuscript Author Manuscript Author Manuscript

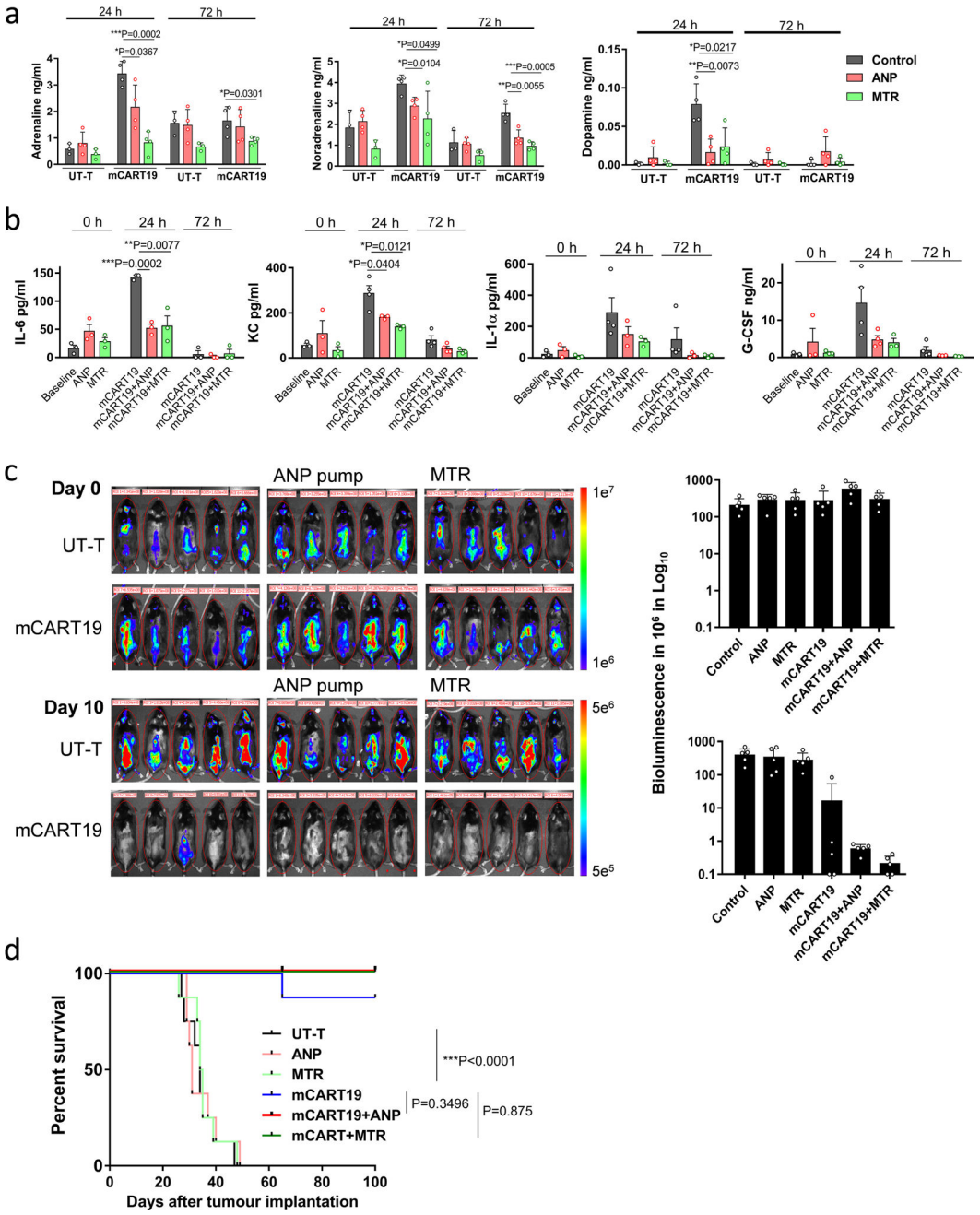

Extended Data Fig. 10 |. MTR and ANP prevent cytokine release in syngeneic Eμ-ALL model without compromising anti-tumour efficacy.

a, **b**, Circulating catecholamines (left to right, $n = 3, 4, 3, 4, 4, 4, 3, 4, 3, 4, 4, 4$ per column/graph) (**a**) and murine cytokines IL-6 ($n = 3$ per column), KC ($n = 3, 3, 3, 4, 3, 3, 4, 4, 3$ per column), IL-1α ($n = 3, 3, 3, 4, 3, 3, 4, 3, 3$ per column) and G-CSF ($n = 3, 3, 3, 4, 4, 3, 4, 3, 3$ per column) (**b**), assessed at 24 and 72 h after mCART19 injection. Data are presented as means ± s.d. with individual data points shown, analysed by two-tailed *t*-test. **c**, BLI was performed before and 10 days after mCART19 cell injection, with or without ANP and MTR pre-treatment ($n = 5$ animals per group). BLI radiance was used to quantify the tumour

Author Manuscript Author Manuscript Author Manuscript Author Manuscript

burden during the treatment course (right). **d**, Percentage survival of Eμ-ALL-mice after mCART19 cell transfer (n = 8 mice per group). Survival differences were analysed by two-sided log-rank test.

Acknowledgements

We thank N. Minton, C. Brayton, K. Kammers, D. Pardoll, Z. Li, E. Watson, C. Thoburn, S. Roy and N. Forbes-McBean for scientific and technical support. This work was supported by NINDS R25NS065729 (V.S.), NCI 1K08CA230179–01 (V.S.), Francis S. Collins Scholar Program (V.S.), DHART-SPORE IN4689861JHU (V.S.), 1R03CA178118–01A1 (R.-Y.B.), BVD (S.Z, R.-Y.B.), the Virginia and D.K. Ludwig Fund for Cancer Research (N.P., K.W.K., B.V., S.Z.), the BKI at Johns Hopkins, and CA062924 (S.Z.).

References

1. van der Poll T, van de Veerdonk FL, Scicluna BP & Netea MG The immunopathology of sepsis and potential therapeutic targets. Nat. Rev. Immunol 17, 407–420 (2017). [PubMed: 28436424]
2. Hansel TT, Kropshofer H, Singer T, Mitchell JA & George AJ The safety and side effects of monoclonal antibodies. Nat. Rev. Drug Discov 9, 325–338 (2010). [PubMed: 20305665]
3. Rommelfanger DM et al. The efficacy versus toxicity profile of combination virotherapy and TLR immunotherapy highlights the danger of administering TLR agonists to oncolytic virus-treated mice. Mol. Ther 21, 348–357 (2013). [PubMed: 23011032]
4. Maude SL, Barrett D, Teachey DT & Grupp SA Managing cytokine release syndrome associated with novel T cell-engaging therapies. Cancer J 20, 119–122 (2014). [PubMed: 24667956]
5. Parker BS, Rautela J & Hertzog PJ Antitumour actions of interferons: implications for cancer therapy. Nat. Rev. Cancer 16, 131–144 (2016). [PubMed: 26911188]
6. Agrawal N et al. Bacteriolytic therapy can generate a potent immune response against experimental tumors. Proc. Natl Acad. Sci. USA 101, 15172–15177 (2004). [PubMed: 15471990]
7. Peters van Ton AM, Kox M, Abdo WF & Pickkers P Precision immunotherapy for sepsis. Front. Immunol 9, 1926 (2018). [PubMed: 30233566]
8. Weber GF et al. Interleukin-3 amplifies acute inflammation and is a potential therapeutic target in sepsis. Science 347, 1260–1265 (2015). [PubMed: 25766237]
9. Vollmar AM The role of atrial natriuretic peptide in the immune system. Peptides 26, 1086–1094 (2005). [PubMed: 15911076]
10. Kuehne SA & Minton NP ClosTron-mediated engineering of *Clostridium*. Bioengineered 3, 247–254 (2012). [PubMed: 22750794]
11. Burke JR et al. BMS-345541 is a highly selective inhibitor of I kappa B kinase that binds at an allosteric site of the enzyme and blocks NF-kappa B-dependent transcription in mice. J. Biol. Chem 278, 1450–1456 (2003). [PubMed: 12403772]
12. Johnson JD et al. Catecholamines mediate stress-induced increases in peripheral and central inflammatory cytokines. Neuroscience 135, 1295–1307 (2005). [PubMed: 16165282]
13. Flierl MA et al. Phagocyte-derived catecholamines enhance acute inflammatory injury. Nature 449, 721–725 (2007). [PubMed: 17914358]
14. Shaked I et al. Transcription factor Nr4a1 couples sympathetic and inflammatory cues in CNS-recruited macrophages to limit neuroinflammation. Nat. Immunol 16, 1228–1234 (2015). [PubMed: 26523867]
15. Clausen BE, Burkhardt C, Reith W, Renkawitz R & Förster I Conditional gene targeting in macrophages and granulocytes using LysMcre mice. Transgenic Res 8, 265–277 (1999). [PubMed: 10621974]
16. Zheng JH et al. Two-step enhanced cancer immunotherapy with engineered *Salmonella typhimurium* secreting heterologous flagellin. Sci. Transl. Med 9, eaak9537 (2017). [PubMed: 28179508]
17. Surbatovic M et al. Cytokine profile in severe Gram-positive and Gram-negative abdominal sepsis. Sci. Rep 5, 11355 (2015). [PubMed: 26079127]

Author Manuscript Author Manuscript Author Manuscript Author Manuscript

18. Sevmis S et al. OKT3 treatment for steroid-resistant acute rejection in kidney transplantation. Transplant. Proc 37, 3016–3018 (2005). [PubMed: 16213290]
19. Neelapu SS et al. Chimeric antigen receptor T-cell therapy - assessment and management of toxicities. Nat. Rev. Clin. Oncol (2017).
20. Giavridis T et al. CAR T cell-induced cytokine release syndrome is mediated by macrophages and abated by IL-1 blockade. Nat. Med 24, 731–738 (2018). [PubMed: 29808005]
21. Norelli M et al. Monocyte-derived IL-1 and IL-6 are differentially required for cytokine-release syndrome and neurotoxicity due to CAR T cells. Nat. Med 24, 739–748 (2018). [PubMed: 29808007]
22. Gill S et al. Preclinical targeting of human acute myeloid leukemia and myeloablation using chimeric antigen receptor-modified T cells. Blood 123, 2343–2354 (2014). [PubMed: 24596416]
23. Ninomiya S et al. Tumor indoleamine 2,3-dioxygenase (IDO) inhibits CD19-CAR T cells and is downregulated by lymphodepleting drugs. Blood 125, 3905–3916 (2015). [PubMed: 25940712]
24. Wunderlich M et al. A xenograft model of macrophage activation syndrome amenable to anti-CD33 and anti-IL-6R treatment. JCI Insight 1, e88181 (2016). [PubMed: 27699249]
25. Flierl MA et al. Upregulation of phagocyte-derived catecholamines augments the acute inflammatory response. PLoS One 4, e4414 (2009). [PubMed: 19212441]
26. Bao JY, Huang Y, Wang F, Peng YP & Qiu YH Expression of α-AR subtypes in T lymphocytes and role of the α-ARs in mediating modulation of T cell function. Neuroimmunomodulation 14, 344–353 (2007). [PubMed: 18463421]

References

27. Jackson CR et al. Retinal dopamine mediates multiple dimensions of light-adapted vision. J. Neurosci 32, 9359–9368 (2012). [PubMed: 22764243]
28. Corrodi H & Hanson LC Central effects of an inhibitor of tyrosine hydroxylation. Psychopharmacologia 10, 116–125 (1966). [PubMed: 5982985]
29. Bettegowda C et al. The genome and transcriptomes of the anti-tumor agent *Clostridium novyi*-NT. Nat. Biotechnol 24, 1573–1580 (2006). [PubMed: 17115055]
30. Lofton CE, Newman WH & Currie MG Atrial natriuretic peptide regulation of endothelial permeability is mediated by cGMP. Biochem. Biophys. Res. Commun 172, 793–799 (1990). [PubMed: 2173580]
31. Zhang X, Goncalves R & Mosser DM The isolation and characterization of murine macrophages. Curr. Protoc. Immunol 10.1002/0471142735.im1401s83 (2008).
32. Rittirsch D, Flierl MA & Ward PA Harmful molecular mechanisms in sepsis. Nat. Rev. Immunol 8, 776–787 (2008). [PubMed: 18802444]
33. Berahovich R et al. FLAG-tagged CD19-specific CAR-T cells eliminate CD19-bearing solid tumor cells in vitro and in vivo. Front. Biosci 22, 1644–1654 (2017).
34. Davila ML, Kloss CC, Gunset G & Sadelain M CD19 CAR-targeted T cells induce long-term remission and B cell aplasia in an immunocompetent mouse model of B cell acute lymphoblastic leukemia. PLoS One 8, e61338 (2013). [PubMed: 23585892]
35. Lee J, Sadelain M & Brentjens R Retroviral transduction of murine primary T lymphocytes. Methods Mol. Biol 506, 83–96 (2009). [PubMed: 19110621]

Author Manuscript
Author Manuscript
Author Manuscript
Author Manuscript

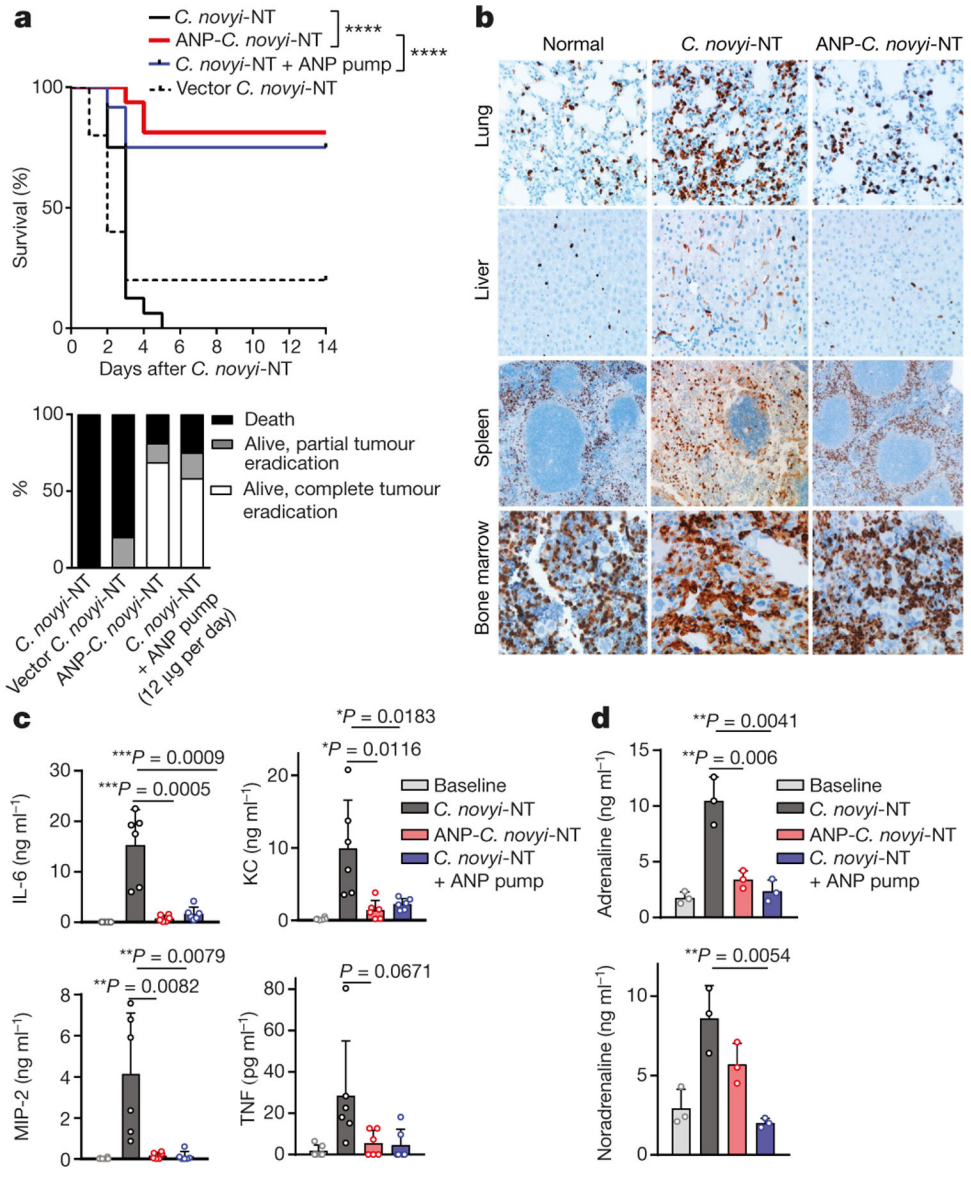

Fig. 1 |. ANP reduces mortality.

a, Kaplan–Meier curve (top panel) and therapeutic response (bottom panel) of ANP-*C. novyi*-NT ($n = 16$) compared to *C. novyi*-NT ($n = 16$), *C. novyi*-NT with ANP via osmotic pump ($n = 12$) and vector *C. novyi*-NT control ($n = 5$). Statistical survival differences were evaluated by two-sided log-rank test. **** $P \leq 0.0001$. **b**, Representative anti-CD11b-antibody-stained sections from the lungs, liver, spleen and bone marrow of mice treated with *ANP-C. novyi*-NT ($n = 3$) and *C. novyi*-NT ($n = 3$) compared to normal controls ($n = 2$). **c**, Plasma levels of indicated cytokines ($n = 6$ independent samples per group) 36 h after spore injection. **d**, Corresponding plasma levels of adrenaline and noradrenaline 36 h after *C. novyi*-NT, ANP-*C. novyi*-NT and *C. novyi*-NT plus ANP pump compared to normal controls ($n = 3$ per group). Data are presented as mean ± s.d. with individual data points shown, analysed by two-tailed *t*-test (**c**, **d**).

Author Manuscript Author Manuscript Author Manuscript Author Manuscript

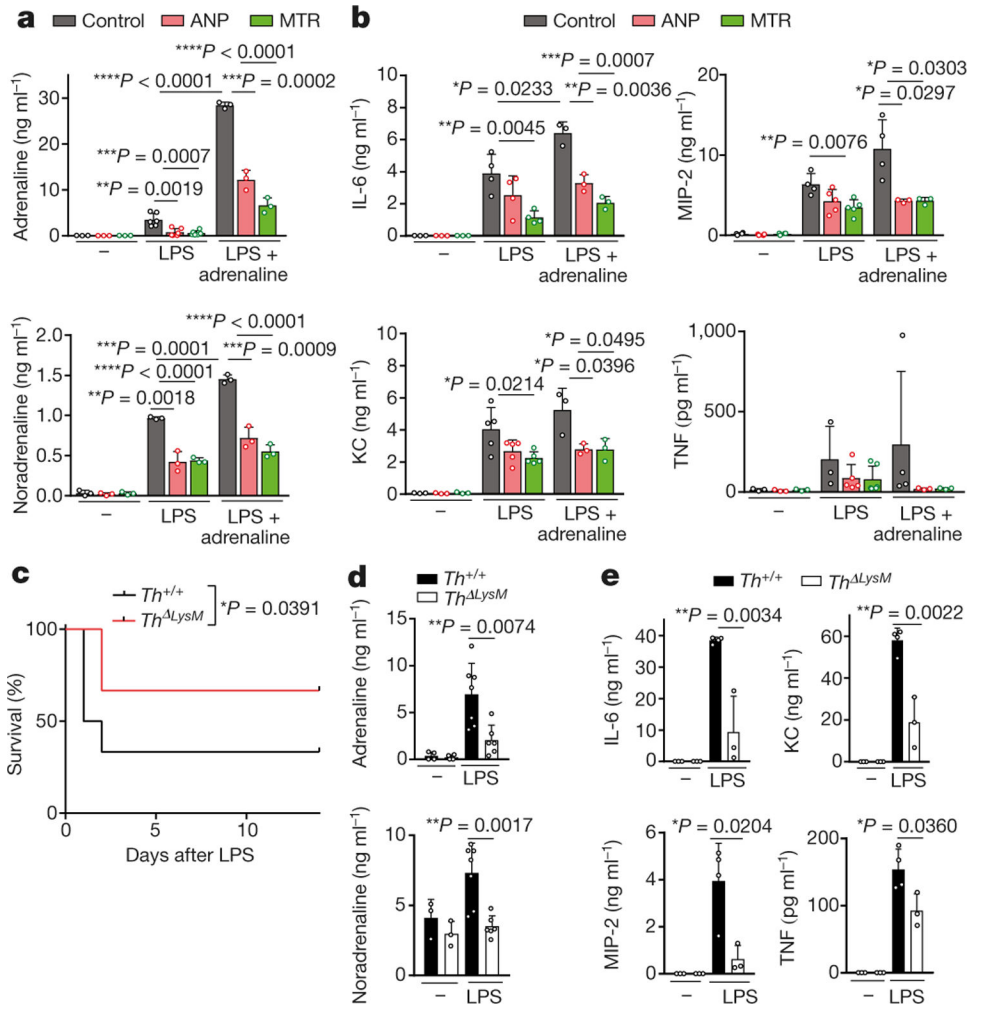

Fig. 2 |. Catecholamine production in myeloid cells is essential for cytokine release.

a, Peritoneal macrophages were pre-incubated with ANP or MTR for 10 min and then stimulated with LPS (50 μg ml^{-1}) or a combination of LPS and adrenaline (15 ng ml^{-1}) in vitro. Shown are the levels of adrenaline (left to right, n = 3, 3, 3, 6, 6, 6, 3, 3, 3 per column) and noradrenaline (n = 3) in the supernatant after 24 h. **b**, Corresponding cytokines from macrophage culture supernatants: IL-6 (n = 3, 3, 3, 4, 4, 4, 3, 3, 3), MIP-2 (n = 4, 4, 4, 4, 5, 5, 4, 3, 3), KC (n = 3, 3, 3, 5, 5, 5, 3, 3, 3) and TNF (n = 3, 3, 3, 3, 5, 6, 4, 3, 3). **c**, Survival of $Th^{+/+}$ and $Th^{\Delta LysM}$ mice treated with LPS and analysed with two-sided log-rank test (n = 12; 6 male, 6 female). **d**, **e**, Plasma levels of adrenaline (n = 4, 4, 7, 6) and noradrenaline (n = 3, 3, 7, 6) (**d**) and indicated cytokines (n = 3, 3, 4, 3) (**e**) at baseline and 24 h after LPS treatment in $Th^{+/+}$ or $Th^{\Delta LysM}$ mice. Data are presented as mean ± s.d. with individual data points shown, analysed by two-tailed t-test (**a**, **b**, **d**, **e**).

Author Manuscript Author Manuscript Author Manuscript Author Manuscript

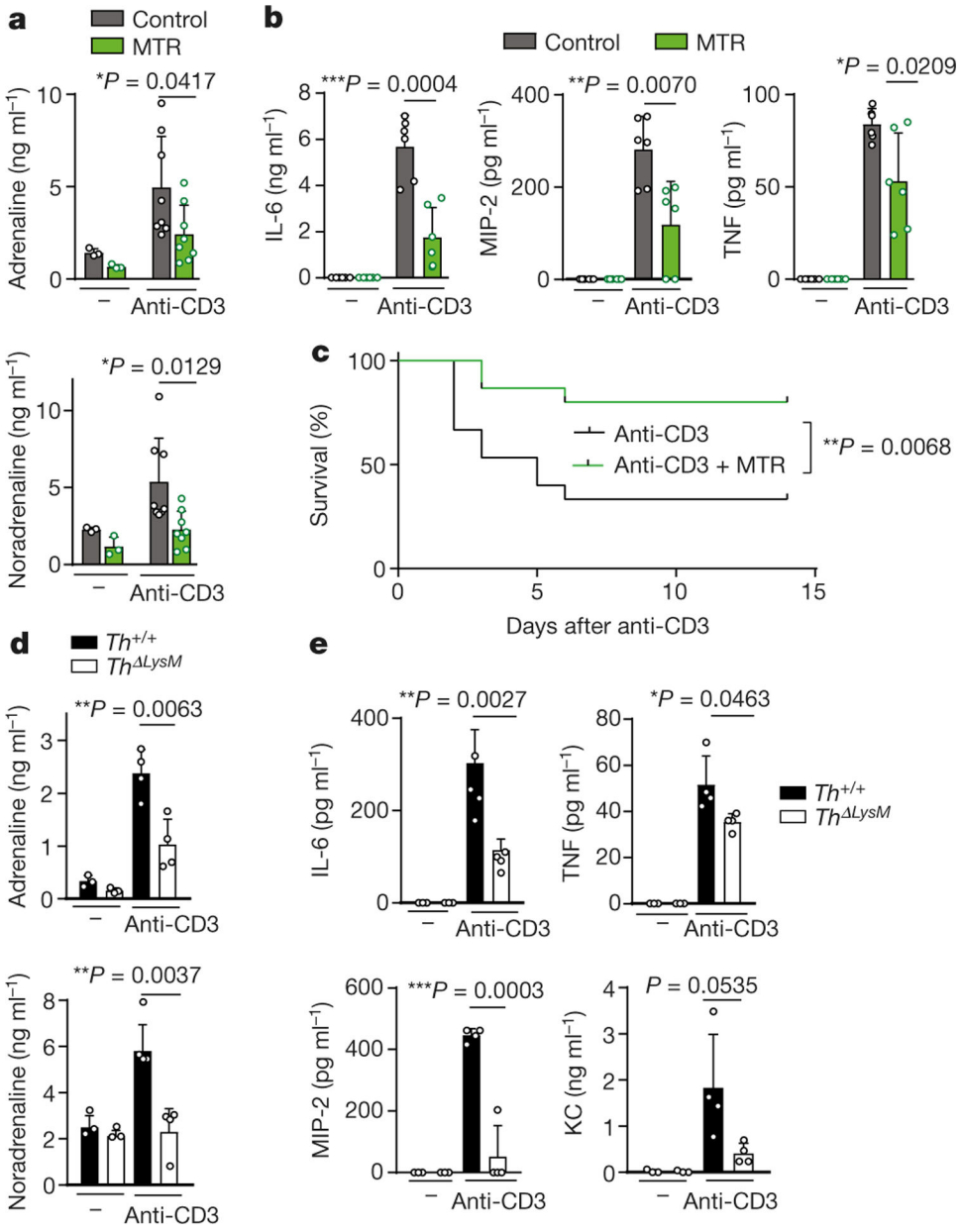

Fig. 3 |. Inhibition of catecholamine synthesis reduces CRS after anti-CD3 treatment.

a, **b**, Levels of adrenaline and noradrenaline (left to right, $n = 3, 3, 8, 8$ independent samples per column) (**a**) and of cytokines ($n = 6$ independent samples) (**b**) measured 24 h after anti-CD3 treatment, with or without MTR. **c**, Survival of BALB/c mice treated with anti-CD3, with or without MTR ($n = 15$ animals); analysed by two-sided log-rank test. **d**, **e**, Levels of adrenaline, noradrenaline ($n = 3, 3, 4, 4$) (**d**) and indicated cytokines ($n = 3, 3, 4, 4$) (**e**) measured 24 h after anti-CD3 treatment in $Th^{+/+}$ or $Th^{\Delta LysM}$ mice. Data are presented as mean ± s.d. with individual data points shown, analysed by two-tailed *t*-test (**a**, **b**, **d**, **e**).

Author Manuscript Author Manuscript Author Manuscript Author Manuscript

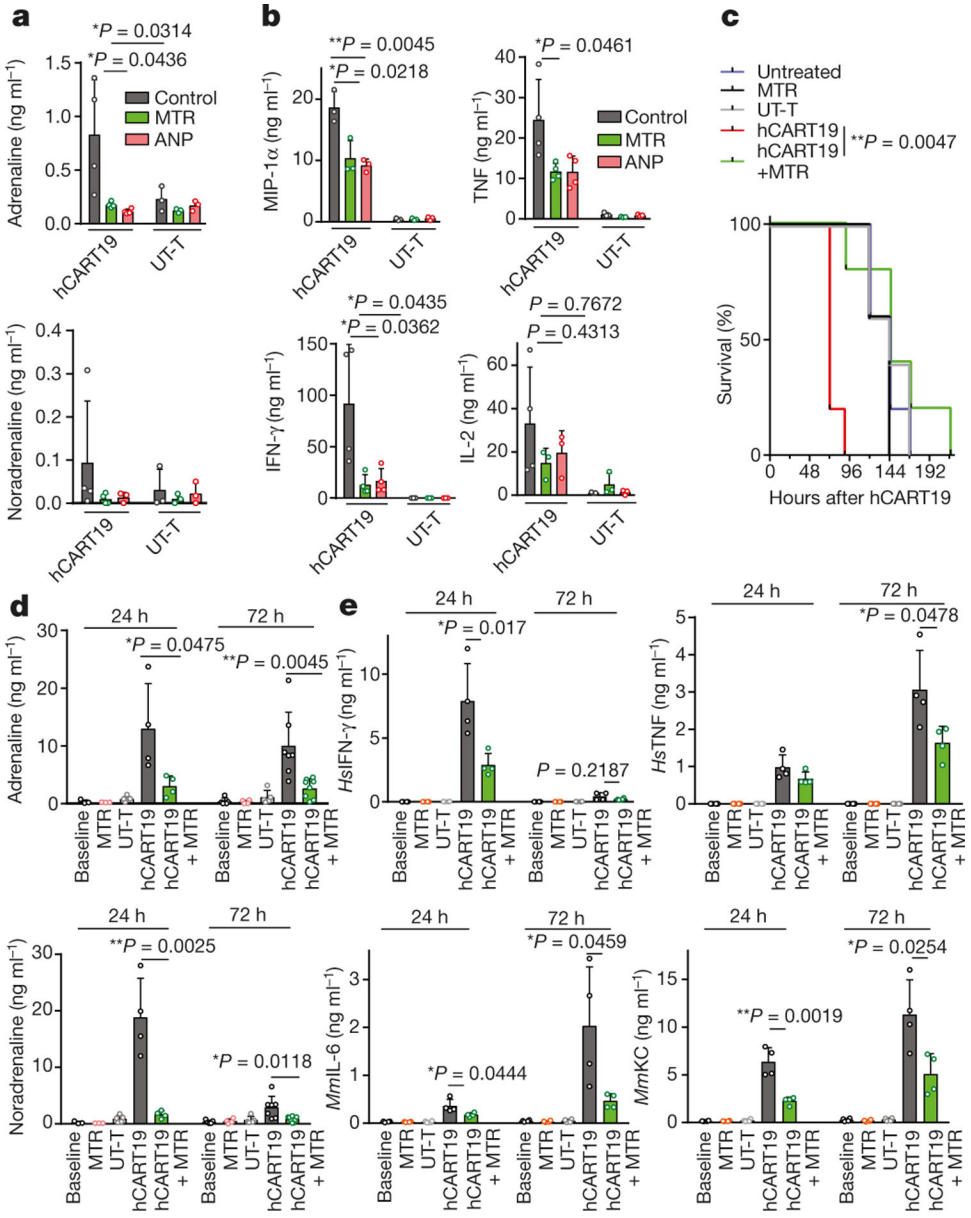

Fig. 4 |. Inhibition of catecholamine synthesis reduces cytokine release induced by hCART19 in vitro and in vivo.

a, **b**, Levels of adrenaline (left to right, $n = 4, 4, 4, 3, 3, 3$ per column) and noradrenaline ($n = 4, 4, 3, 3, 3, 3$) (**a**) and corresponding cytokines MIP-1α ($n = 3$), TNF ($n = 4, 4, 4, 3, 3, 3$), IFN-γ ($n = 4, 4, 4, 3, 3, 3$) and IL-2 ($n = 4, 3, 3, 3, 3, 3$) (**b**) in the supernatant 24 h after incubation of Raji cells with hCART19 or UT-T (ratio 1:5), with or without MTR or ANP. **c**, Survival of Raji-bearing NSGS mice with high tumour burden, treated with 1.5×10^7 hCART19, with or without MTR pre-treatment compared to UT-T, MTR and no treatment ($n = 5$ mice per group). Survival differences were evaluated by two-sided log-rank test. **d**, **e**, Levels of circulating adrenaline and noradrenaline ($n = 3, 3, 5, 4, 4, 5, 4, 5, 7, 8$) (**d**) and of indicated circulating mouse and human cytokines ($n = 4$ samples per group) (**e**), assessed 24 and 72 h after administration of hCART19 with or without MTR in comparison to controls.

Author Manuscript Author Manuscript Author Manuscript Author Manuscript

Data are presented as mean ± s.d. with individual data points shown, analysed by two-tailed *t*-test (**a**, **b**, **d**, **e**).

Author Manuscript Author Manuscript Author Manuscript Author Manuscript

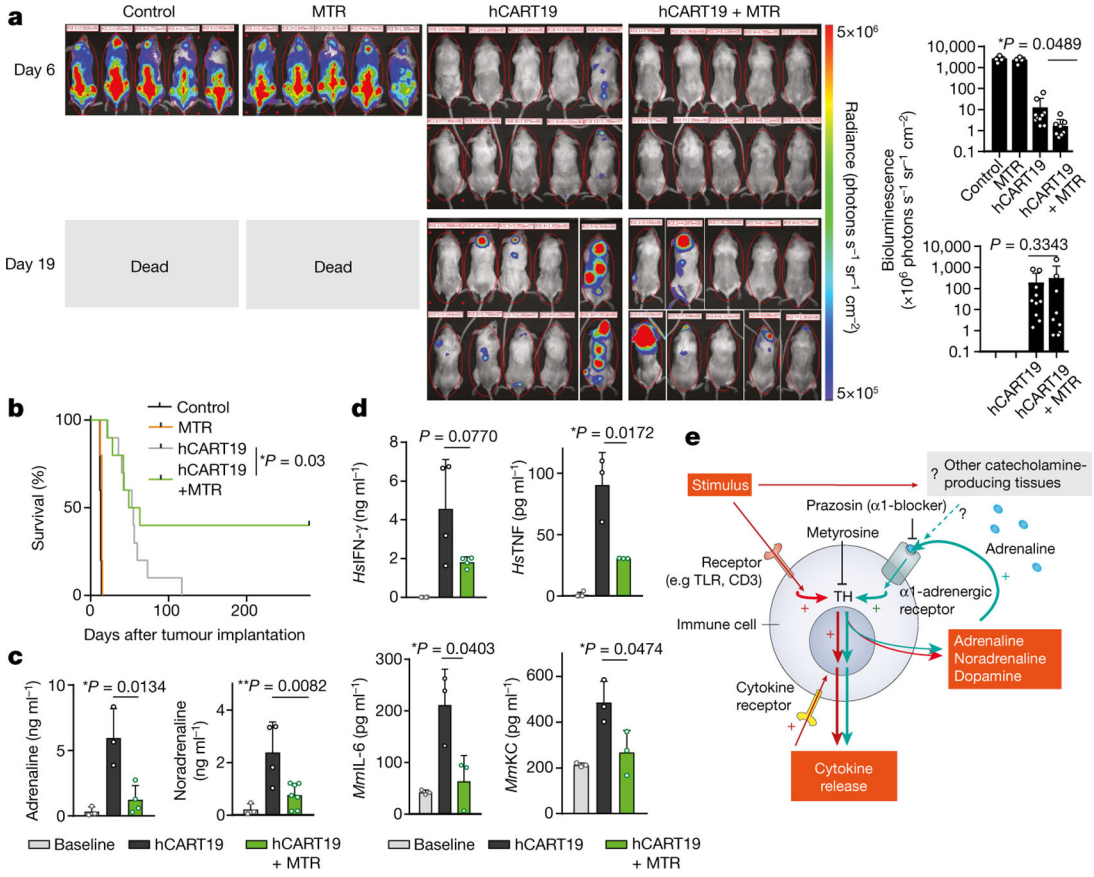

Fig. 5 |. Inhibition of catecholamine synthesis with MTR does not impair the therapeutic response of hCART19.

a, Serial bioluminescence imaging (BLI) of Raji-bearing NSGS mice (low tumour burden)at day 6 and 19 after treatment with 1.5×10^7 hCART19, with or without MTR ($n = 10$ mice per group) compared to control (UT-T), with or without MTR ($n = 5$ mice per group). BLI counts were used to quantify the tumour burden during the treatment course (right). Statistical differences were evaluated by one-tailed *t*-test. **b**, Corresponding Kaplan–Meier curve of Raji-bearing NSGS mice with low tumour burden, treated with 1.5×10^7 hCART19, with or without MTR pre-treatment ($n = 10$ mice per group) in comparison to control (UT-T), with or without MTR ($n = 5$ mice per group). Survival differences were analysed by weighted log-rank test (see Methods). **c**, **d**, Levels of plasma adrenaline ($n = 3$, 3, 4 per column) and noradrenaline ($n = 3$, 4, 7) (**c**) and *Hs*IFN-γ ($n = 4$), *Hs*TNF ($n = 4$, 3, 3), and mouse cytokines *Mm*IL-6 ($n = 3$) and *Mm*KC ($n = 3$) (**d**), assessed 72 h after hCART19 treatment. Data are presented as mean ± s.d. with individual data points shown, analysed by two-tailed *t*-test. **e**, Scheme showing how inhibition of the catecholamine pathway may reduce CRS. TLR, toll-like receptor.